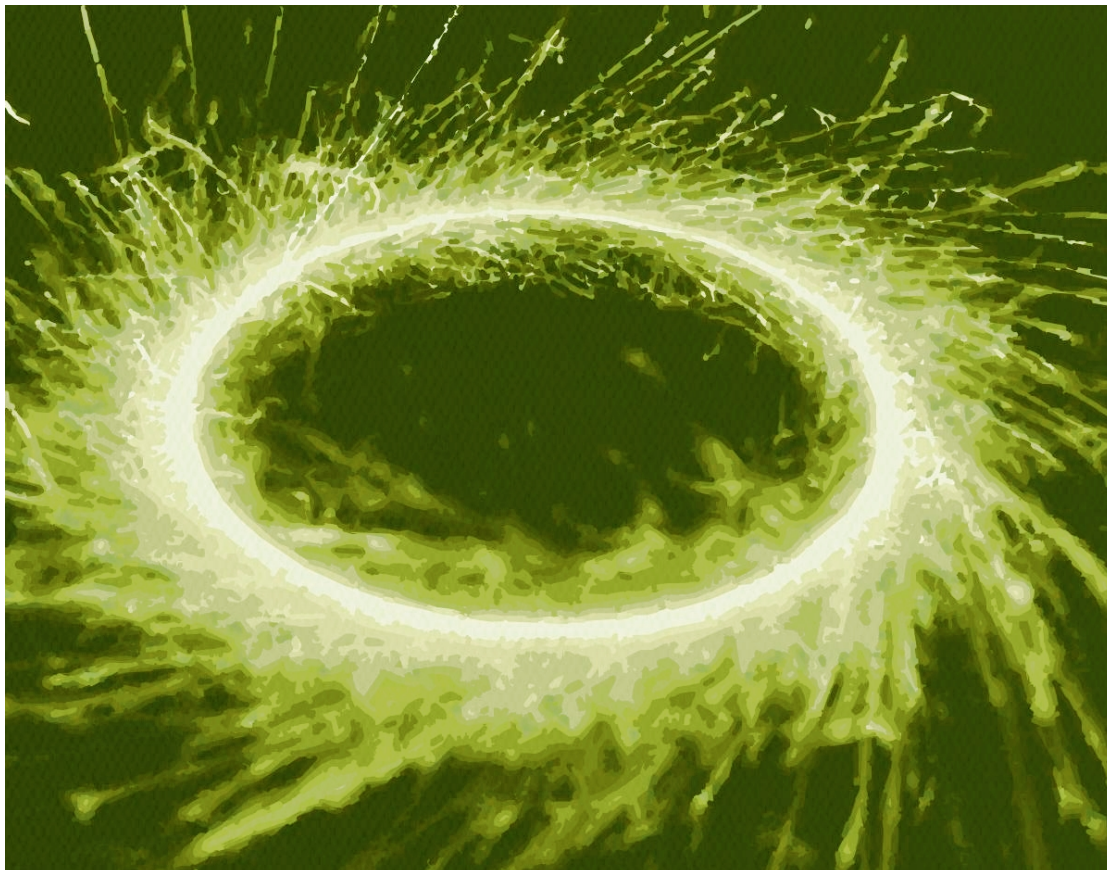


# Luminosity determination for the 2012 CMS pp data



Monika Grothe  
( U Wisconsin)

# Luminosity and how one measures it

$$R = \sigma L$$

A characteristic of accelerator operation that relates what one can measure (the rate, R) to the physics (the cross section,  $\sigma$ ) behind it

- Luminosity needs to be known to
  - determine absolute cross sections from the observed rate for a process of interest
  - monitor the accelerator performance
- Ingredients for all LHC experiments:
  - Online monitoring in real time, with both the experiment and the machine as customers
  - Offline determination with high precision, with physics analyses as customers
  - Absolute calibration via dedicated Van-der-Meer LHC runs

Measuring luminosity at the LHC is highly collaborative undertaking, concerted effort of all experiments and of the machine together

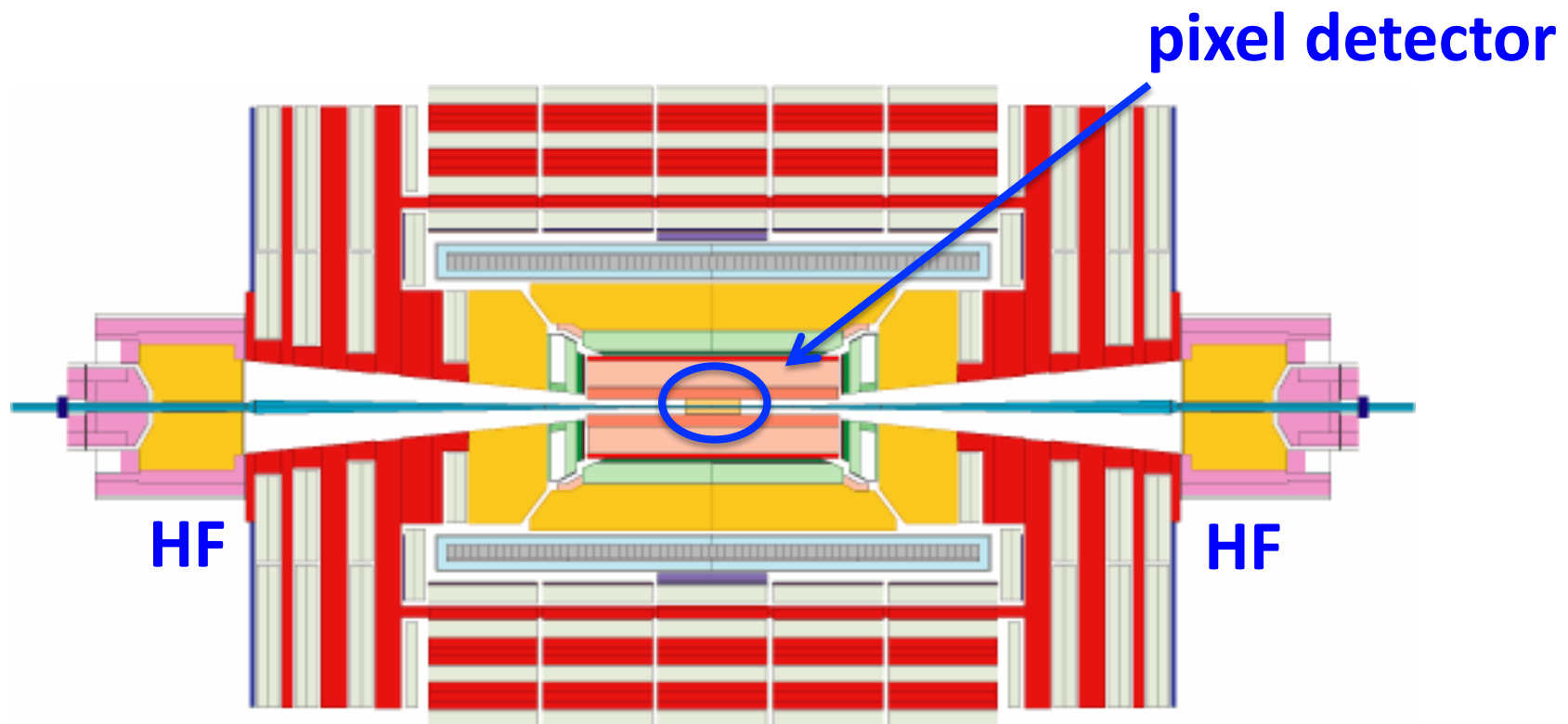
Information exchange and development of shared methods and tools in the LHC Luminosity Monitoring and Calibration working group (LLCMWG)

# Outline

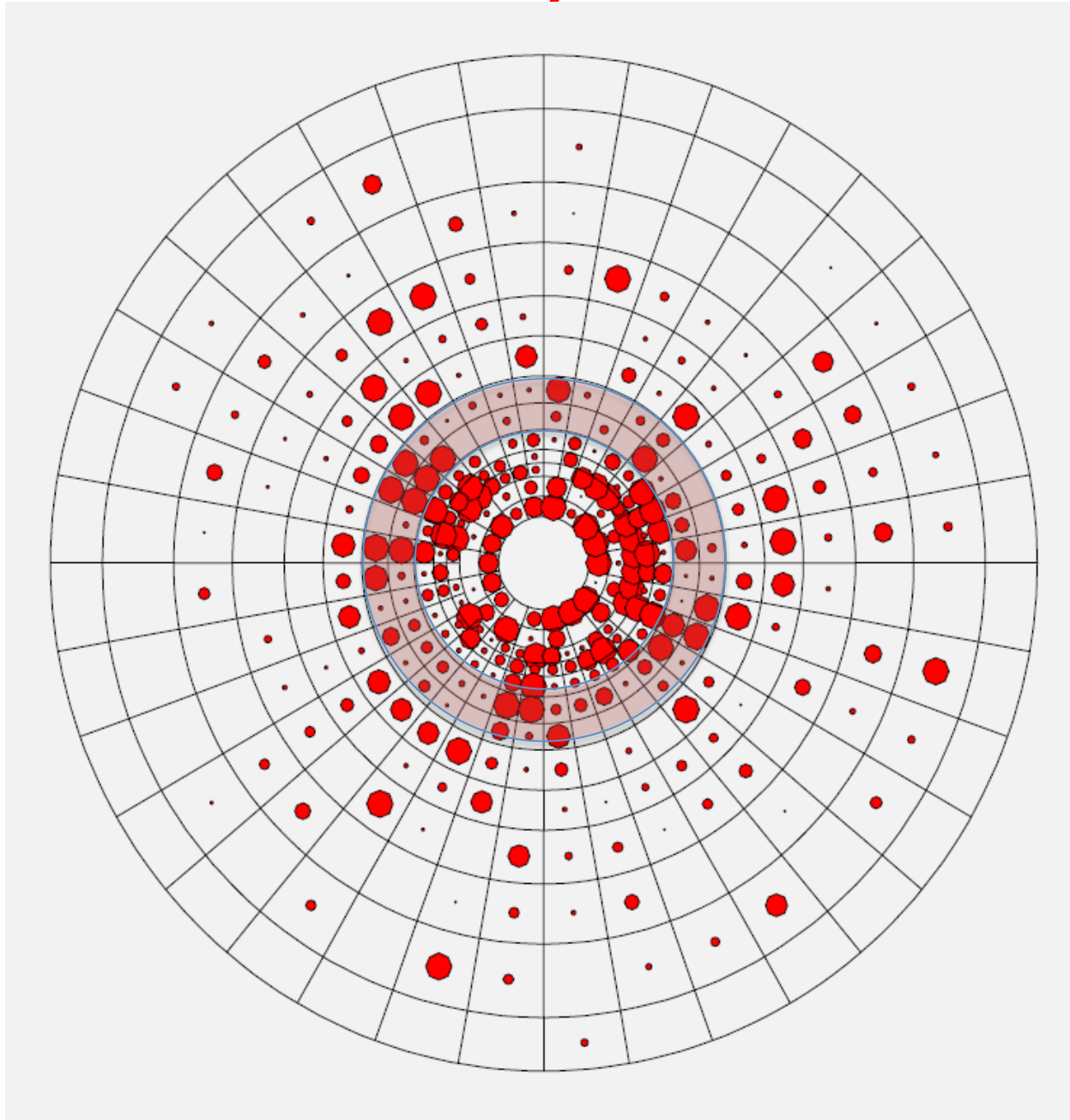
- Luminometers in CMS
- Online luminosity monitoring in 2012 in CMS with HF empty tower counting
- Absolute luminosity calibration via Van-der-Meer scans
  - Method basics
  - VdM scans in 2012: Evolution of our understanding
- Calibration for 2012 pp data via pixel cluster counting
  - Analysis of the November 2012 VdM scan campaign
  - Corrections: absolute beam intensity calibration, ghosts and satellites, length-scale calibration, orbit drift, beam-beam deflection, dynamics beta correction
- Summary and outlook beyond LS1 (BCM1F, pixel-luminosity telescope)

# Luminometers used in 2012 in CMS

- Use as luminometers processes with well-understood and well-behaved rates
- Luminometers in 2012 pp running
  - HF empty tower counting: Online, offline, VdM
  - pixel cluster counting: Online DQM, offline, VdM
  - vertex counting: Offline



# Luminosity measurement with HF



$$\mu = \frac{\sigma L}{f}$$

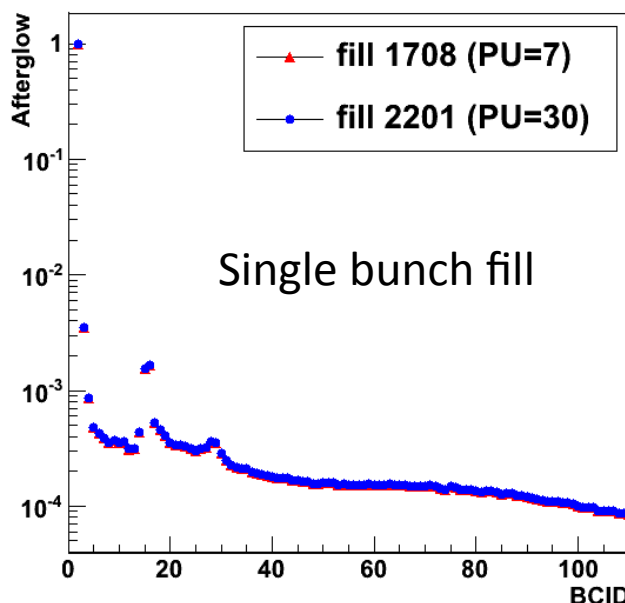
No. of interactions is  
Poisson with mean  $\mu$

$$\langle f_0 \rangle = e^{-(1-p)\mu}$$

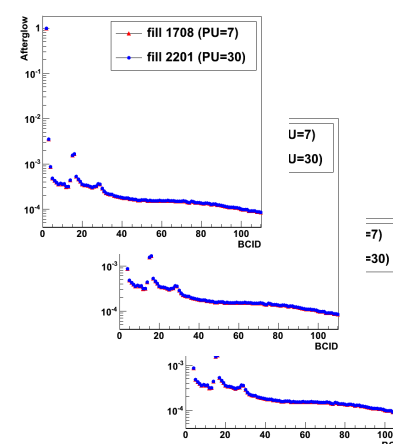
$$-\ln \langle f_0 \rangle = (1 - p)\mu$$

# Correction of HF “raw” luminosity: Afterglow correction

- One of the features of the HF photomultipliers is a characteristic afterpulse
  - Its shape is stable and independent of the luminosity
  - however for fills with many bunches it biases the luminosity measurement
- A deconvolution correction is applied depending on the filling scheme for a given run
  - Correction significantly improves luminosity leakage into non-colliding bunches
  - as well as the value of the luminosity measured in the colliding bunches

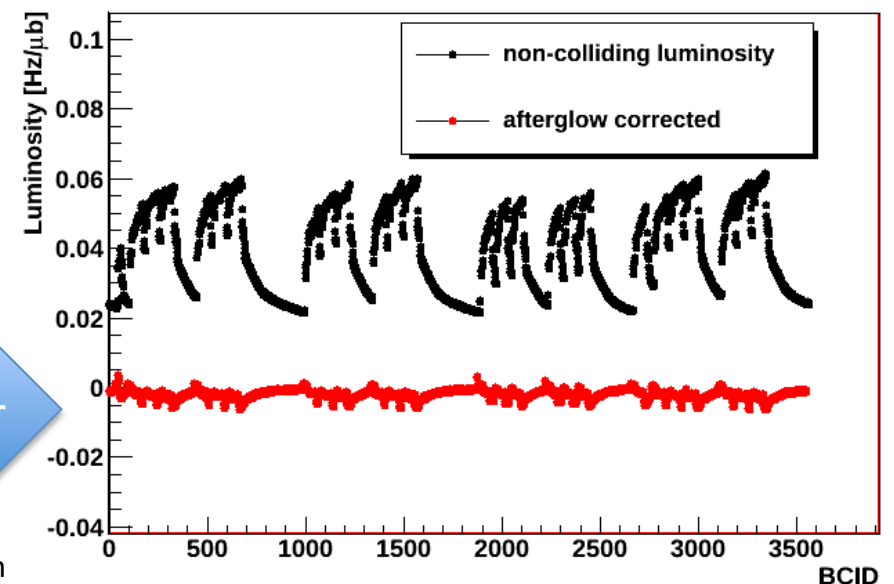


Single bunch fill



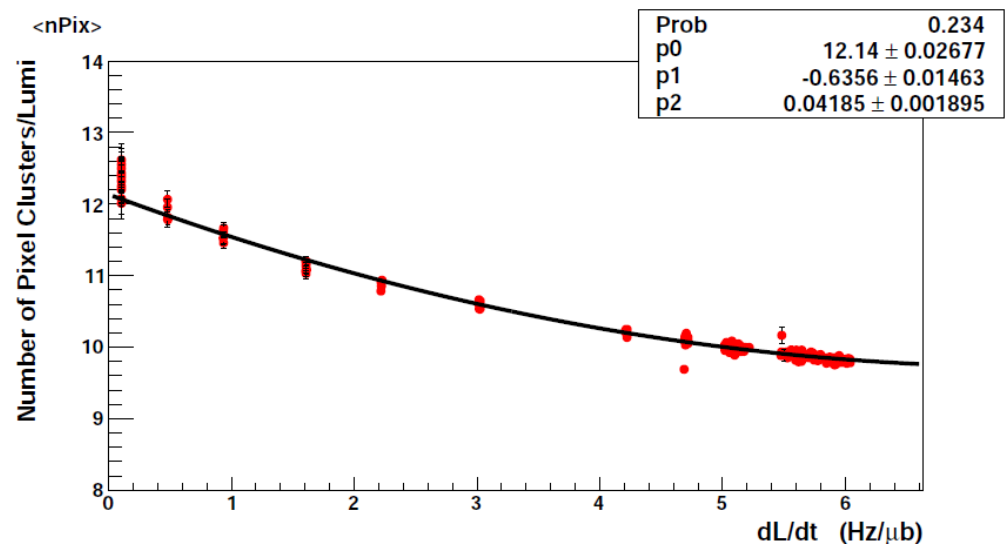
Deconvolution corr

Luminosity determination



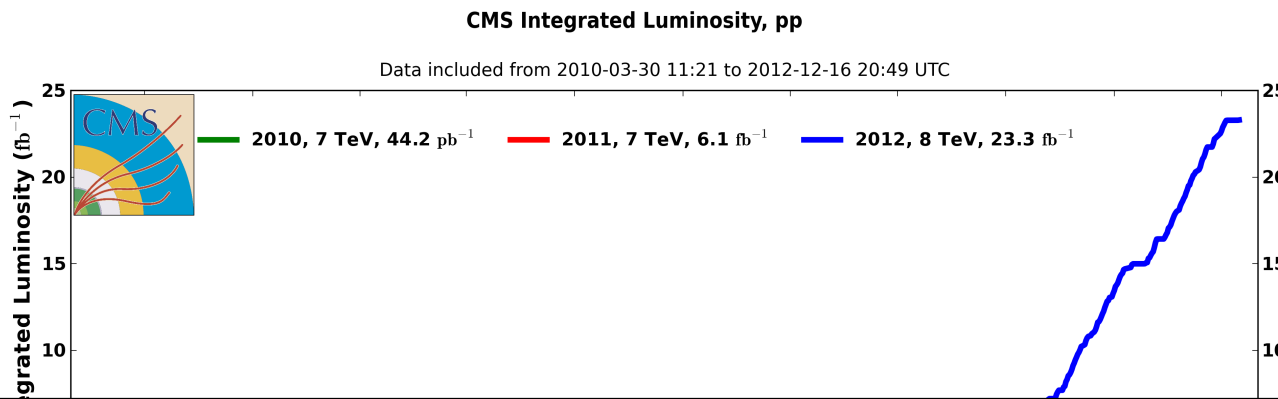
# Correction of HF “raw” luminosity: Non-linearity effects

- Non-linearity with pile-up:
  - Particles from multiple collisions might hit the same HF tower.
  - These **subthreshold** hits cause non-linearities
- Pixel cluster X section vs bunch-by-bunch instantaneous luminosity, measured during a dedicated high pile-up scan in Oct 2011
  - Deviation from flat line describes the non-linearity
  - Correction from 2011 also applied to 2012 HFlumi measurement
- Non-linearity caused by HF response changes:
  - Comparison of HF lumi with lumi from pixel cluster and vertex counting showed significant calibration changes (4-6% over 2011)
  - Presumably caused by radiation damage in the HF PMTs.
  - Corrected in 2012 by uploading of re-calibrated gains to HF look-up tables several times over 2012

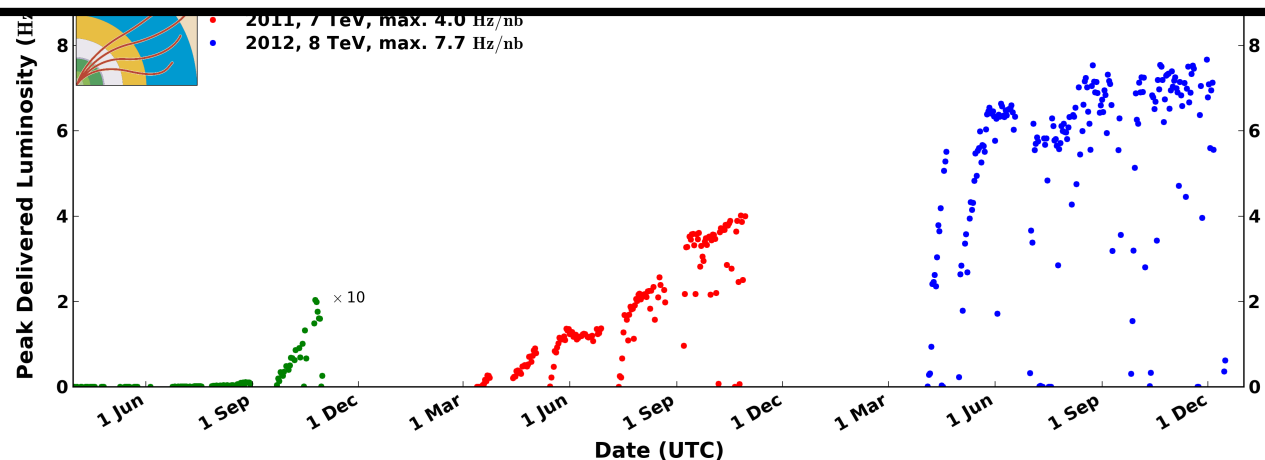


All these effects are corrected for in HFlumi numbers from lumiCalc.  
Gives sufficient accuracy for online and offline monitoring purposes.

# Luminosity monitored by HF in 2012

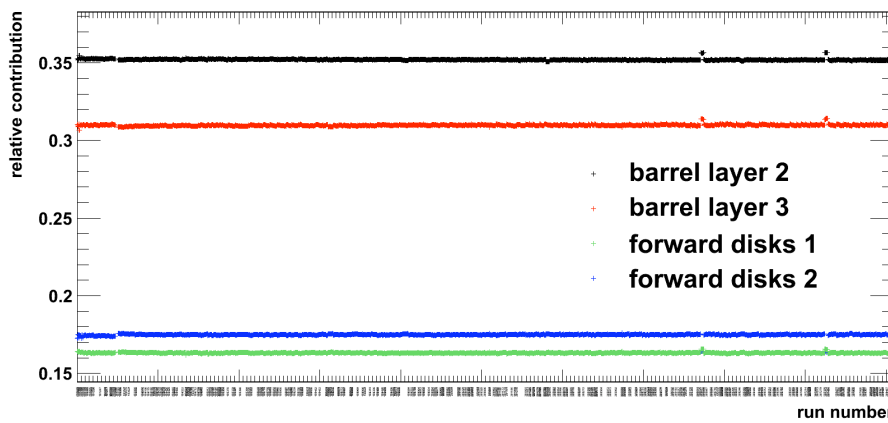
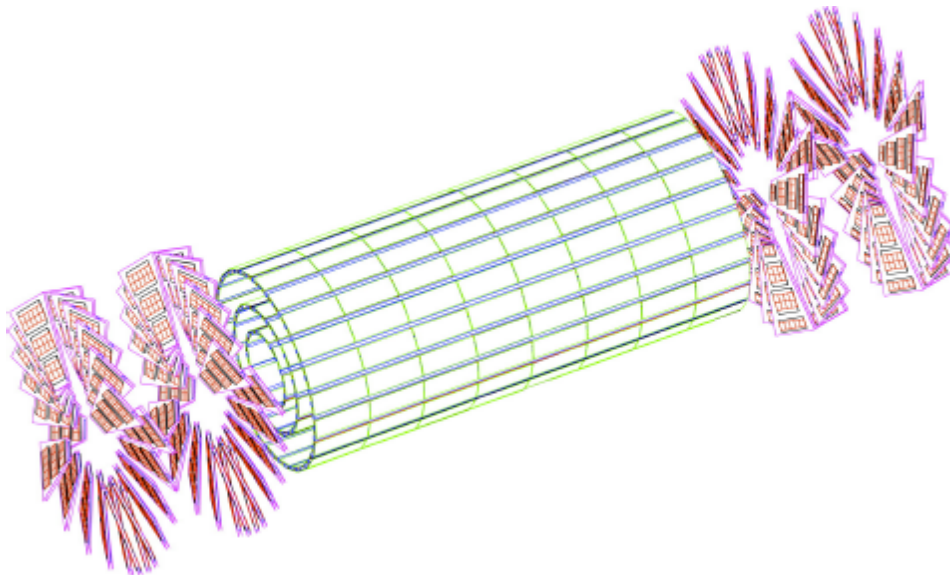


However, for high-precision luminosity determination for physics analyses purposes, we turned to method that is not affected by these non-linearity effects: Pixel cluster counting

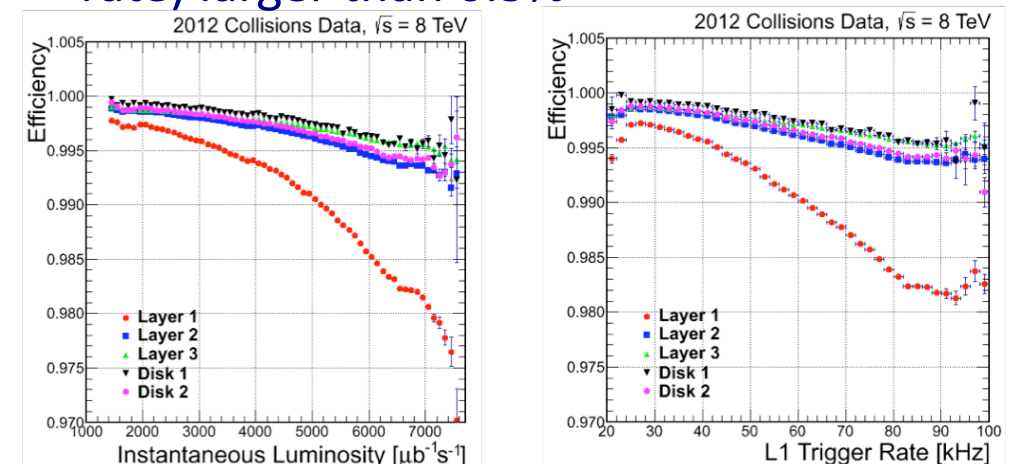


From public CMS lumi page <https://twiki.cern.ch/twiki/bin/view/CMSPublic/LumiPublicResults>

# Luminosity measurement with pixel cluster counting



- Linearity with pile-up: At LHC design luminosity:
  - the occupancy in the pixel detector is on average less than 0.1%
  - the average number of clusters per minimum bias interaction is about 200
  - the average number of pixels per cluster is about 5
- Excellent stability observed in 2012 run
- Innermost barrel pixel layer excluded from cluster counting because of dynamic inefficiencies (due to high L1 rate) larger than 0.5%



# Luminosity measurement with pixel cluster counting (II)

- Define the pixel cluster cross section  $\sigma_{clus}$  as the zero-bias cross section  $\sigma_{zb}$  multiplied by the average number of pixel clusters per zero-bias interaction  $\langle N_{clus} \rangle$
- The luminosity L delivered in any lumi section is then given by:

$$L = \frac{\langle N_{clus} \rangle n_{bx} f_{orb} \Delta t_{LS}}{\sigma_{clus}}$$

- where:
  - $n_{bx}$  is the number of active bunch crossings in the LHC filling scheme used at the time
  - $f_{orb} = 11246$  Hz is the LHC revolution frequency
  - $\Delta t_{LS} = 2^{18}$  orbits = 23.31 s is the duration of a single luminosity section

Used for determination of luminosity offline

Uses special ZeroBias AlCaLumiPixel stream, records just 5 BX

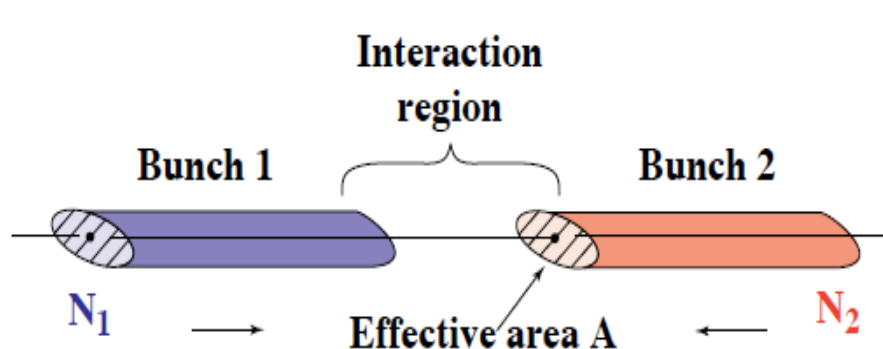
No non-linearity with pile-up and no detector response drifts with time

Afterglow correction needed because of small out-of-time response, probably caused by slight activation in detector material and surrounding

So far: Luminosity monitoring  
But need calibration point to nail  
down absolute calibration

→ Van der Meer scans

# Van der Meer scan method



$$L = \underbrace{N_1 N_2}_\text{No. of protons in beams 1,2} \underbrace{f}_\text{LHC orbit frequency} \underbrace{n_b}_\text{No. of colliding bunches} / \underbrace{A_{\text{eff}}}_\text{effective area}$$

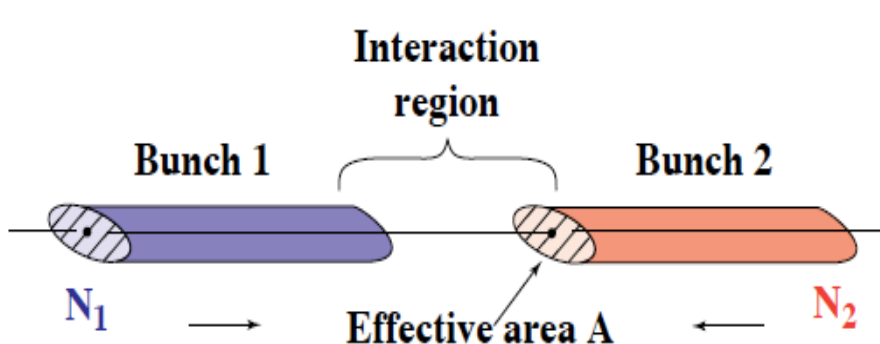
Overlap of the two beam proton densities

$$\begin{aligned} L &= N_1 N_2 f n_b \underbrace{\int \rho_1(x,y) \rho_2(x,y) dx dy}_{\text{assuming factorizability}} \\ &= N_1 N_2 f n_b \int \rho_1(x) \rho_2(x) dx \int \rho_1(y) \rho_2(y) dy \end{aligned}$$

Method pioneered by Simon van der Meer at ISR:

Determine  $A_{\text{eff}}$  by measuring rates when sweeping beams across each other in one coordinate while keeping them heads-on in the other.

# Van der Meer scan method



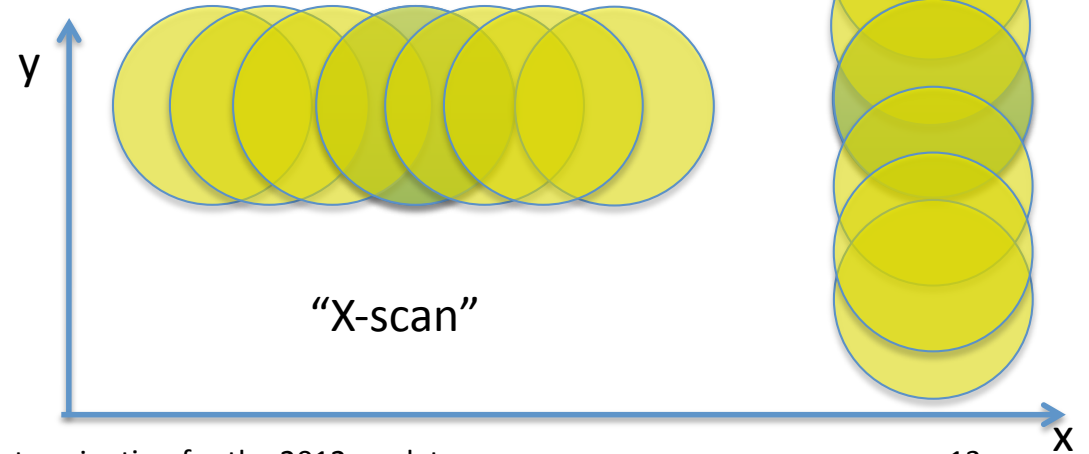
$$L = \underbrace{N_1 N_2}_{\text{No. of protons in beams 1,2}} \underbrace{f}_{\text{LHC orbit frequency}} \underbrace{n_b}_{\text{No. of colliding bunches}} / \underbrace{A_{\text{eff}}}_{\text{effective area}}$$

Overlap of the two beam proton densities

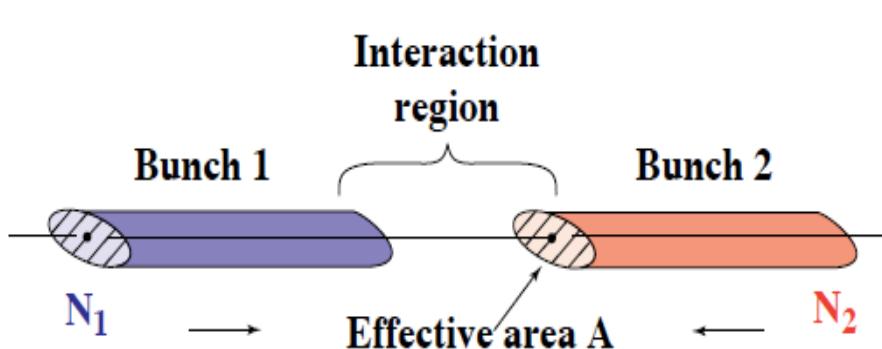
$$L = N_1 N_2 f n_b \underbrace{\int \rho_1(x,y) \rho_2(x,y) dx dy}_{\text{assuming factorizability}}$$

$$= N_1 N_2 f n_b \int \rho_1(x) \rho_2(x) dx \int \rho_1(y) \rho_2(y) dy$$

Method pioneered by Simon van der Meer at ISR: Determine  $A_{\text{eff}}$  by measuring rates when sweeping beams across each other in one coordinate while keeping them heads-on in the other.



# Van der Meer scan method (II)



$$L = \underbrace{N_1 N_2}_{\text{No. of protons in beams 1,2}} \underbrace{f}_{\text{LHC orbit frequency}} \underbrace{n_b}_{\text{No. of colliding bunches}} / \underbrace{A_{eff}}_{\text{effective area}}$$

$$A_{eff} = \frac{\int R(\Delta x) d\Delta x}{R(\Delta x_0)} \frac{\int R(\Delta y) d\Delta y}{R(\Delta y_0)} = \frac{\int R(\Delta x, \Delta y_0) d\Delta x \int R(\Delta x_0, \Delta y) d\Delta y}{R^2(\Delta x_0, \Delta y_0)}$$

This result is independent of the beam shapes, but assumes that the proton densities are factorizable in x and y.

Recall: Rate = Xsec times luminosity

In VdM scan, cross section is the visible part,  $\sigma_{vis}$ , of the inelastic pp cross section,  $\sigma_{inel} \approx 72 \text{ mb}$

$$\sigma_{vis} = \frac{R(\Delta x_0, \Delta y_0)}{L} = \frac{\int R(\Delta x, \Delta y_0) d\Delta x \int R(\Delta x_0, \Delta y) d\Delta y}{N_1 N_2 f n_b R(\Delta x_0, \Delta y_0)}$$

# VdM scan with Gaussian beams

Convolution of two Gaussian beams is itself a Gaussian with width “CapSigma”,  $\Sigma$ .

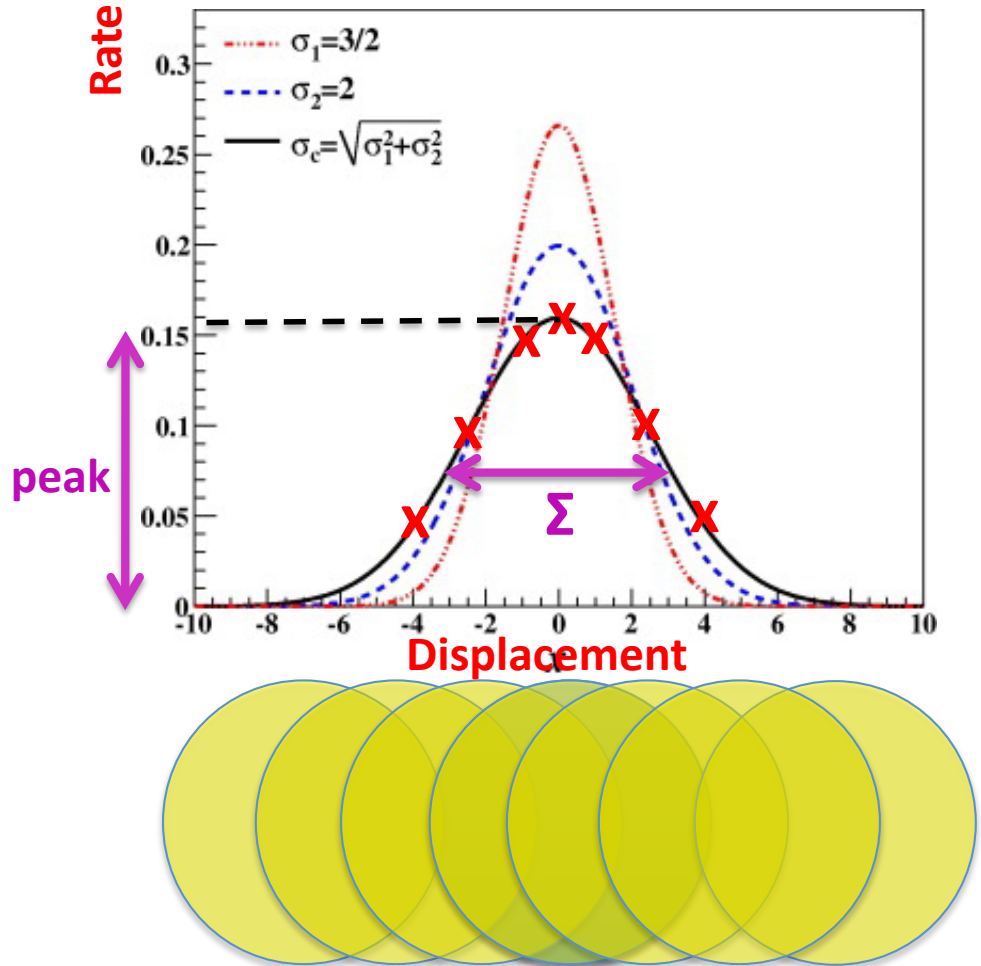
In VdM scan determine:

$\Sigma_x$  and Peak<sub>x</sub> in X-scan  
 $\Sigma_y$  and Peak<sub>y</sub> in Y-scan

$$A_{eff} = 2\pi\Sigma_x\Sigma_y$$

$$\sigma_{vis} = \frac{2\pi \Sigma_X \Sigma_Y}{N_1 N_2 f n_b} \left( \frac{\text{Peak}_X + \text{Peak}_Y}{2} \right)$$

This can be generalized to case of double-Gaussian beams.



# VdM scans in 2012

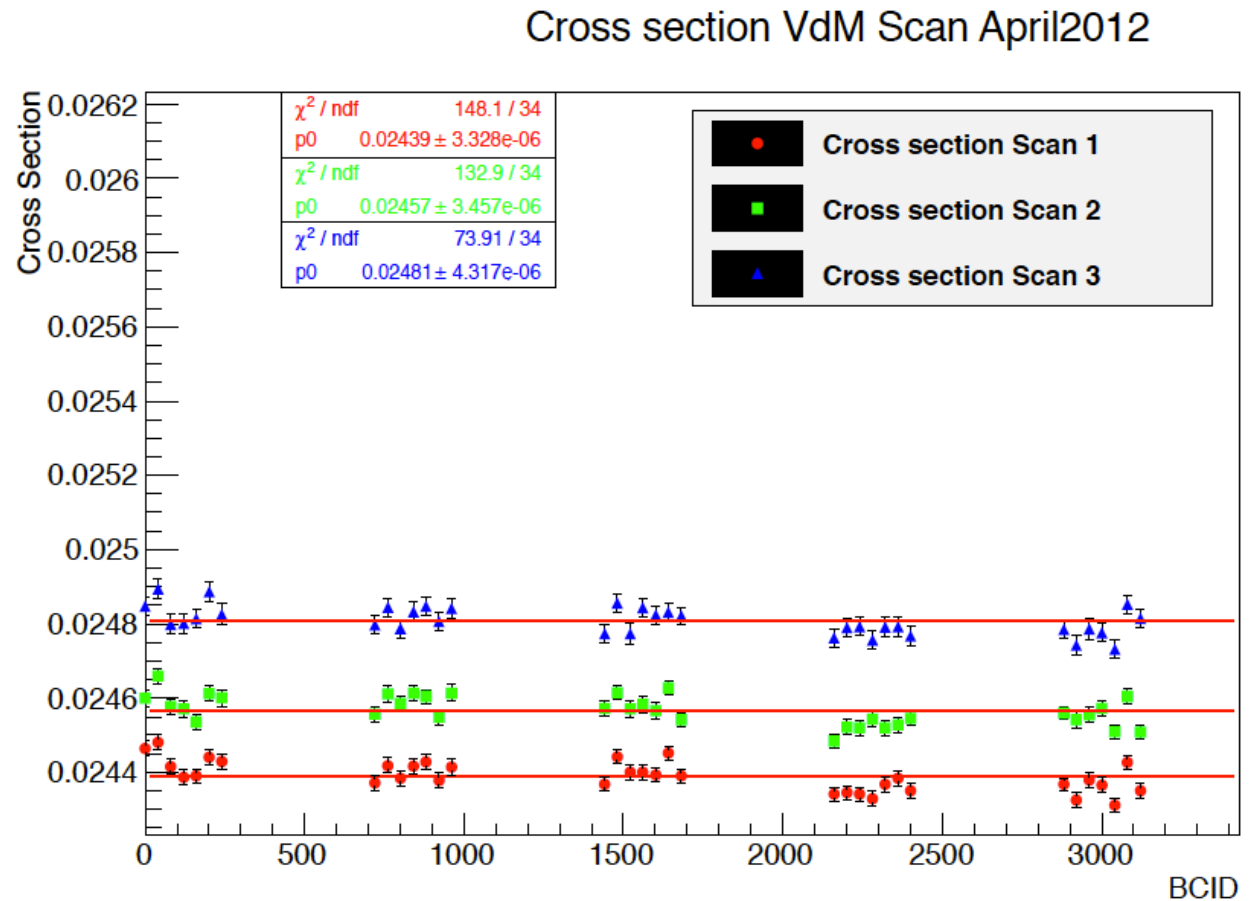
2012 VdM scans	Fill	scans	parameters		
APRIL-2012 LSC	2520	3 times X-Y head-on	Multi_48b_35_3_6_4bpi14inj	$\beta^*=0.6m$	145 $\mu$ rad
APRIL-2012 VDM	2576	length scale calibration	50ns_88b_75_0_60_36bpi4inj	$\beta^*=0.6m$	145 $\mu$ rad
JUNE-2012 VDM-end-of-fill	2710	X-Y head-on	50ns_1380b_1377_0_1274_144bpi12inj	$\beta^*=0.6m$	145 $\mu$ rad
JULY-2012 VDM	2855	3 times X-Y head-on, length scale calibration	Multi_48b_35_3_6_4bpi14inj_b	$\beta^*=11m$	0 $\mu$ rad
	2856	X-Y head-on, offset X-Y by $1.6\sigma$	Multi_48b_35_3_6_4bpi14inj_b	$\beta^*=11m$	0 $\mu$ rad
OCTOBER VDM-end-of-fill	3236	X 30s/point, X 4s/point, Y 30s/point, Y 4s/point, X 4s/point	50ns_1374_1368_0_1262_144bpi12inj	$\beta^*=0.6m$	145 $\mu$ rad
NOVEMBER VDM	3316	X-Y, Y-X head-on, offset X-Y by $1.5\sigma$ , offset X-Y by $3.0\sigma$ , Y-X head-on	Multi_39b_29_2_6_4bpi13inj	$\beta^*=11m$	0 $\mu$ rad

- 5 VdM scan campaigns in 2012, with different beam/machine conditions:
  - 3 in dedicated VdM fills
  - 2 as end-of-fill scans, with nominal physics conditions
- Preliminary calibration used up to Aug 2013 was from HF data of April 2012 campaign, final calibration (see PAS LUM-13-001) is from pixel analysis of Nov 2012 campaign

Will explain in the following why for the final absolute luminosity calibration, we use only the November 2012 VdM scan

# Scan-to-scan variations in VdM campaigns prior to Nov

- Visible Xsec from HFlumi determined from fit to beam overlap shapes for each BCID and for each of the 3 April scans
- Fit function in X and in Y is a double Gaussian in each case
- Shown in % of 72.7 mb
- Scan-to-scan variations are O(2%)
- Pixel analysis in CMS and ATLAS analysis confirm finding

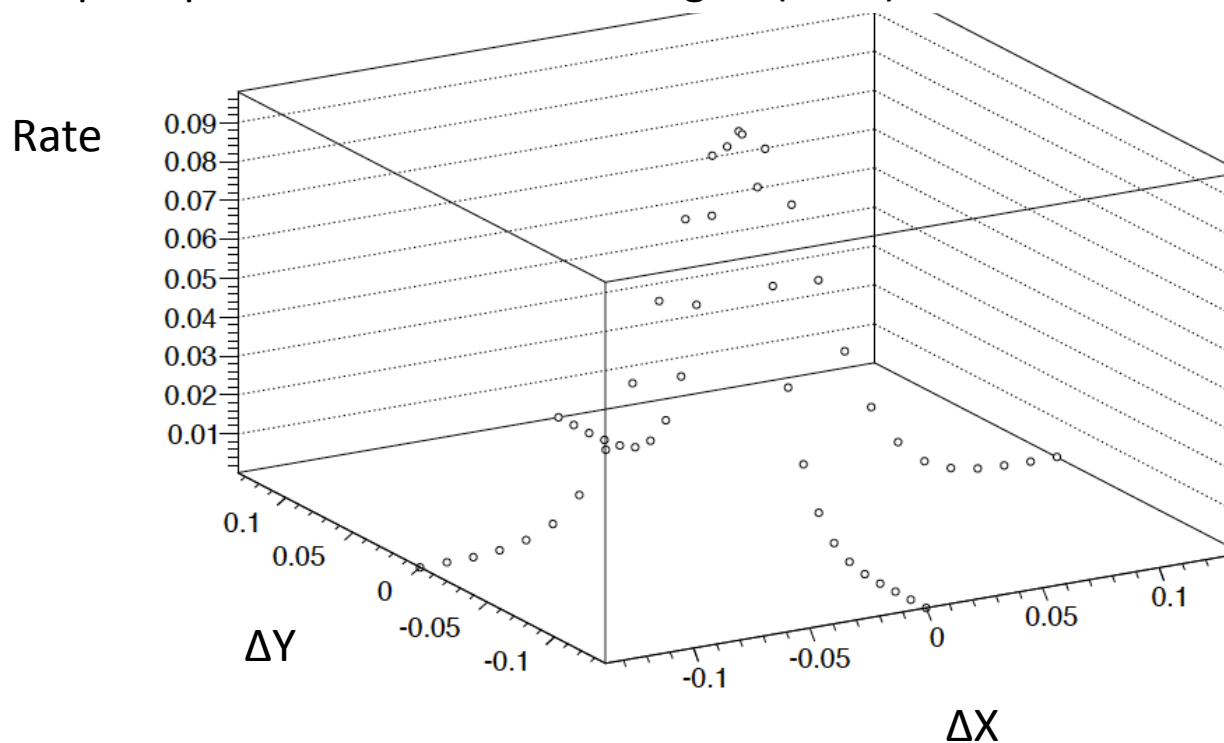


- Scan-to-scan variations are dominant uncertainty on all VdM analyses (including those in ATLAS)
- All analyses appear to observe indications for strong X-Y correlations in the VdM scan data which break the assumption of X-Y factorizability in the VdM method
- Subsequent scan campaigns till Oct did not solve problem

# 1<sup>st</sup> remedy attempt: 2D fits with X-Y correlation

- “1D” fit function (traditional):
  - one double Gaussian plus constant for X scan
  - another double Gaussian plus constant for Y scan
  - disregards possible X-Y correlations

The dots are the data points one actually measures of the full 2D beam-beam overlap shape for one bunch-crossing ID (BCID)



# 1<sup>st</sup> remedy attempt: 2D fits with X-Y correlation

- “1D” fit function (traditional):
  - one double Gaussian plus constant for X scan
  - another double Gaussian plus constant for Y scan
  - disregards possible X-Y correlations
- Alternative “2D” fit function (as proposed by ATLAS)
  - double Gaussian beam shapes where width of the second Gaussian is that one of first Gaussian times a scale factor
  - with very simple form of X-Y correlation (ad hoc assumption)

$$R(x, y) = A \left( f e^{-(x-x_{01})^2/2\sigma_x^2} e^{-(y-y_{01})^2/2\sigma_y^2} + (1-f) e^{-(x-x_{02})^2/2(S_x\sigma_x)^2} e^{-(y-y_{02})^2/2(S_y\sigma_y)^2} \right)$$

— which necessitates:

$$\sigma_{vis} = \frac{\int R(\Delta x, \Delta y_0) d\Delta x \cdot \int R(\Delta x_0, \Delta y) d\Delta y}{\nu N_1 N_2 R(\Delta x_0, \Delta y_0)} \quad \longrightarrow \quad \sigma_{vis} = \frac{\int R(\Delta x, \Delta y) d\Delta x d\Delta y}{\nu N_1 N_2 R(\Delta x_0, \Delta y_0)}$$

Shown in the following:

(Measured rate in HF)/N1N2, where N1, N2 are the beam intensities

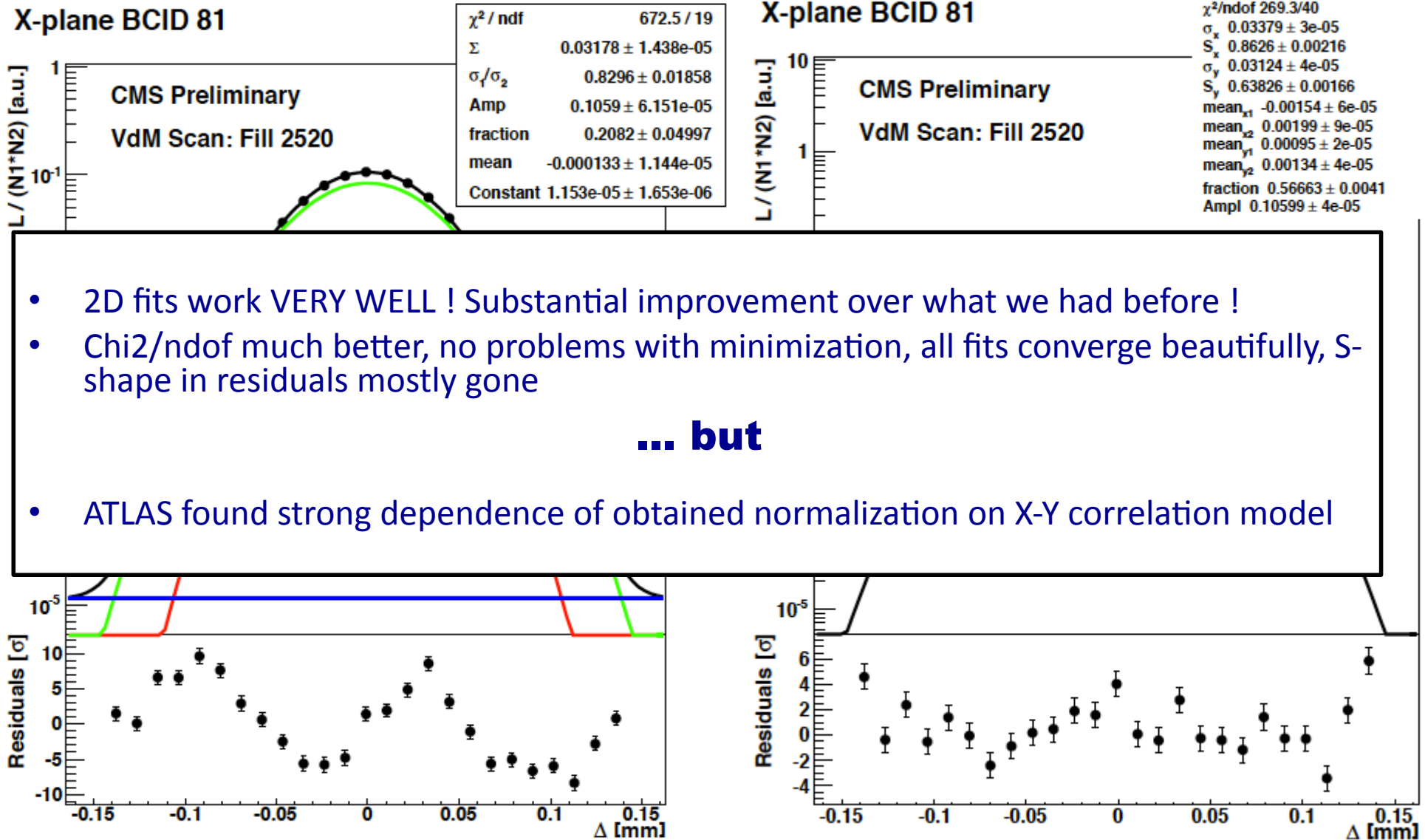
# Correction Jan 2015

- Formula for 2D sigvis is wrong, correct one below
- Furthermore, formula only holds for rates, i.e. when luminometer measures counts per time, as does HF

$$R(x, y) = A \left( f e^{-(x-x_{01})^2/2\sigma_x^2} e^{-(y-y_{01})^2/2\sigma_y^2} + (1-f) e^{-(x-x_{02})^2/2(S_x\sigma_x)^2} e^{-(y-y_{02})^2/2(S_y\sigma_y)^2} \right)$$

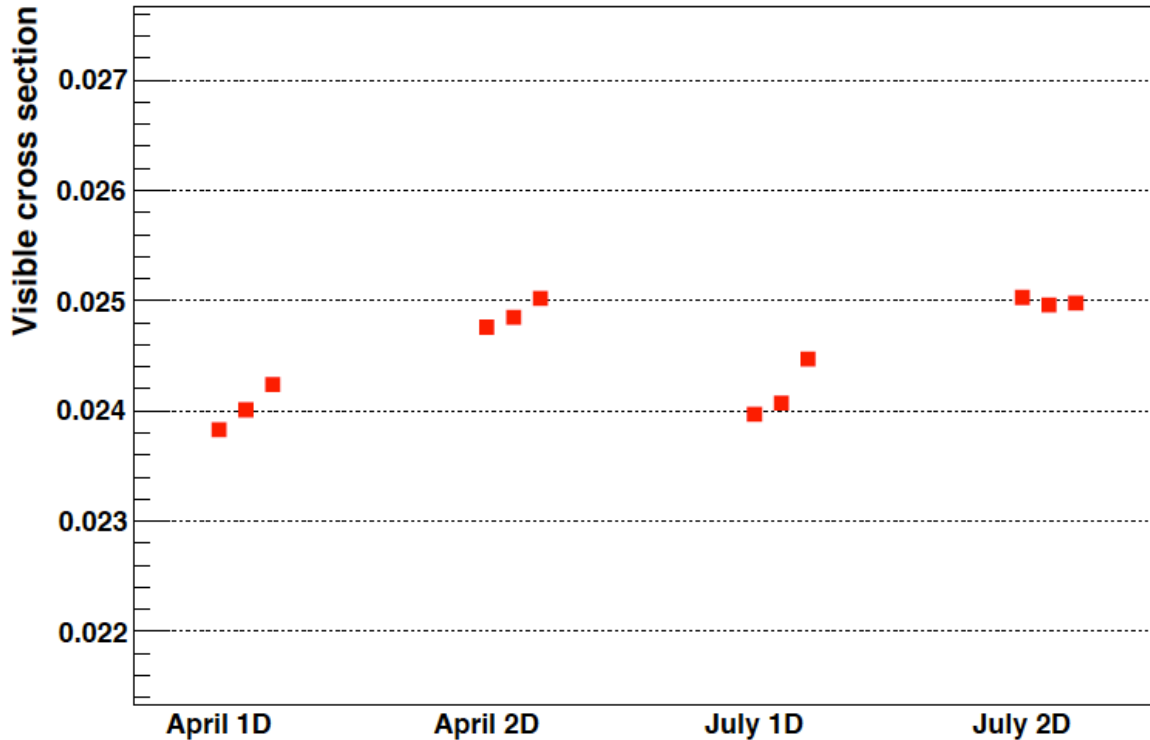
$$\sigma_{vis} = \frac{\int R(\Delta x, \Delta y_0) d\Delta x \cdot \int R(\Delta x_0, \Delta y) d\Delta y}{\nu N_1 N_2 R(\Delta x_0, \Delta y_0)} \quad \longrightarrow \quad \sigma_{vis} = \frac{\int R(\Delta x, \Delta y) d\Delta x d\Delta y}{\nu N_1 N_2}$$

# April VdM scan 1: “1D” left, “2D” right



# Lumi normalization from 1D and 2D fits

HFlumi visible cross section (1D and 2D fit) as function of VdM scan

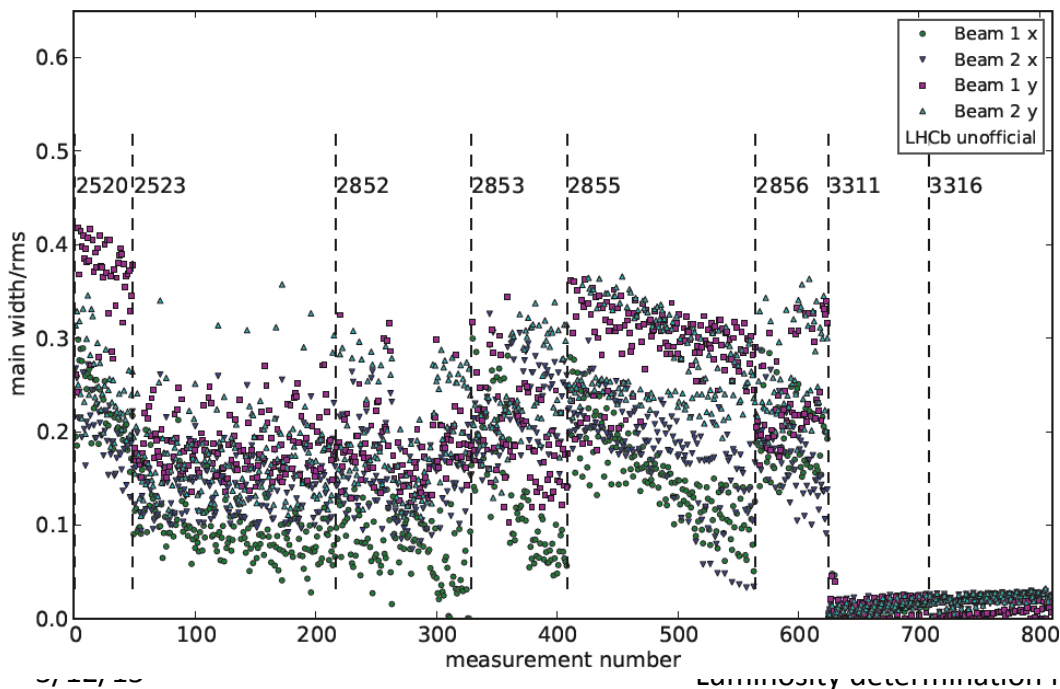


- Shown are HFlumi results from dedicated VdM fills in April and July
- Only scans where the (0,0) position in the non-scanning plane corresponded to heads-on beams
- No correction applied for HF gain changes

- This is currently not understood
- Additional constraints are needed to gain a better understanding of type of X-Y correlations present in the beams (e.g. movement of luminous region during scan, change of width of luminous region during scan)

# 2<sup>nd</sup> remedy attempt: Nov VdM campaign

- Machine carried out special MD to be able to provide beams that were as Gaussian as possible, with as little X-Y correlations as possible
  - $\beta^*=11$ , null crossing angle
  - Octupoles switched off (less non-linear effects)
  - No beam screens
  - Dedicated injection sequence/procedure
- Which indeed resulted in beams in the Nov scans that were beautifully Gaussian and even close to single Gaussian
- Confirmed also by ATLAS and LHCb

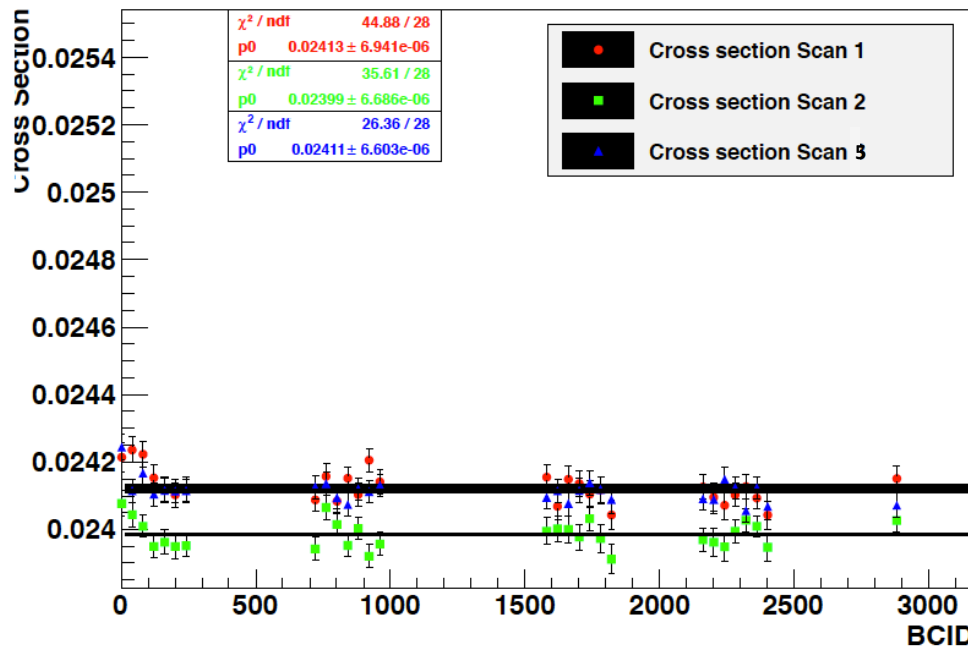


From LHCb, determined from beam-gas data  
For 1D double Gaussian fits  
Shows contribution of Gaussian with least weight to overall width

Note: X-Y correlations are possible only if both beams are at least double Gaussian , i.e. no X-Y correlations possible for single Gaussian beam(s)

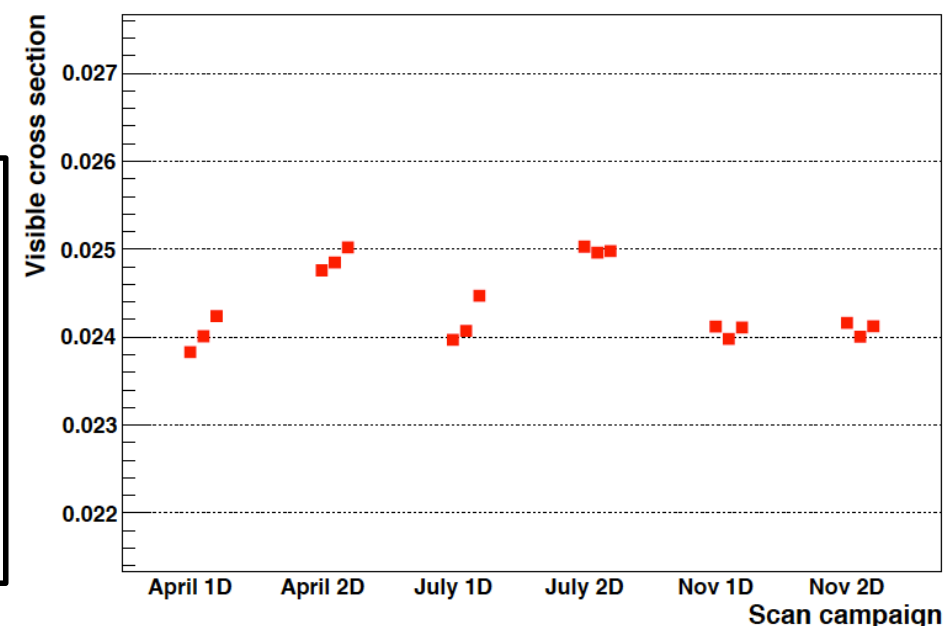
# Nov 2012 scans: Visible X section from HFlumi

Cross section VdM Scan Nov2012



- Scan-to-scan variations of O(0.5%)
- Compare to O(2%) in April and July scans
- Calculated with the 1D, uncorrelated fit method
- Results of 1D and 2D fit methods in good agreement

HFlumi visible cross section (1D and 2D fit) as function of VdM scan



- Nov VdM campaign with goal of delivering beams that are as close as possible to single Gaussian was a full success
- Derive final luminosity calibration for 2012 pp data from Nov VdM campaign only

# Analysis of the November VdM scan campaign

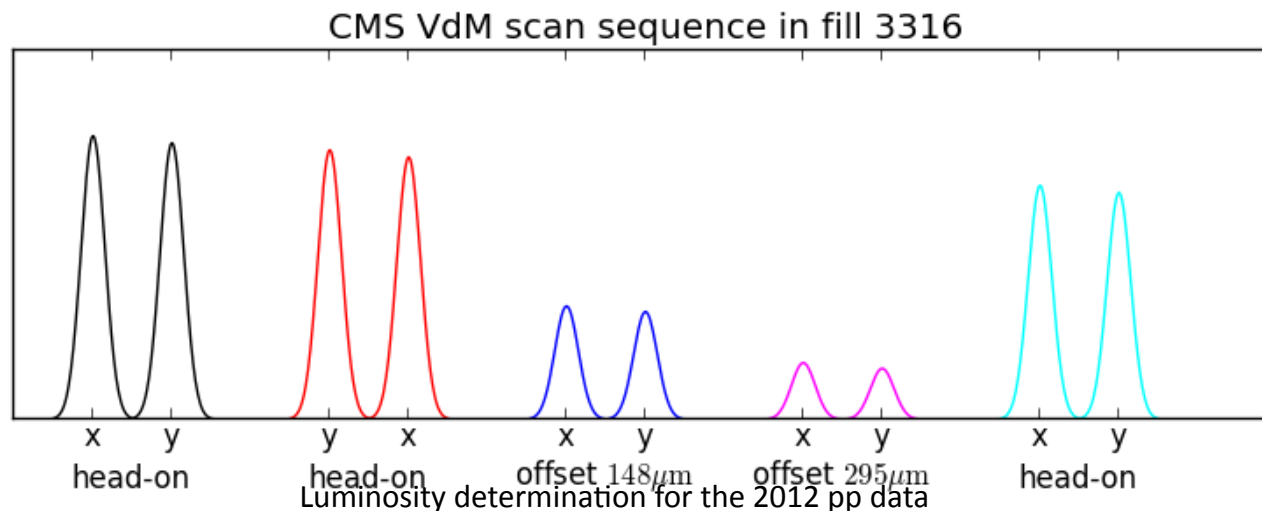
Strategy:

Use pixel cluster counting to determine calibration (systematic effects better under control) for full 2012 pp dataset

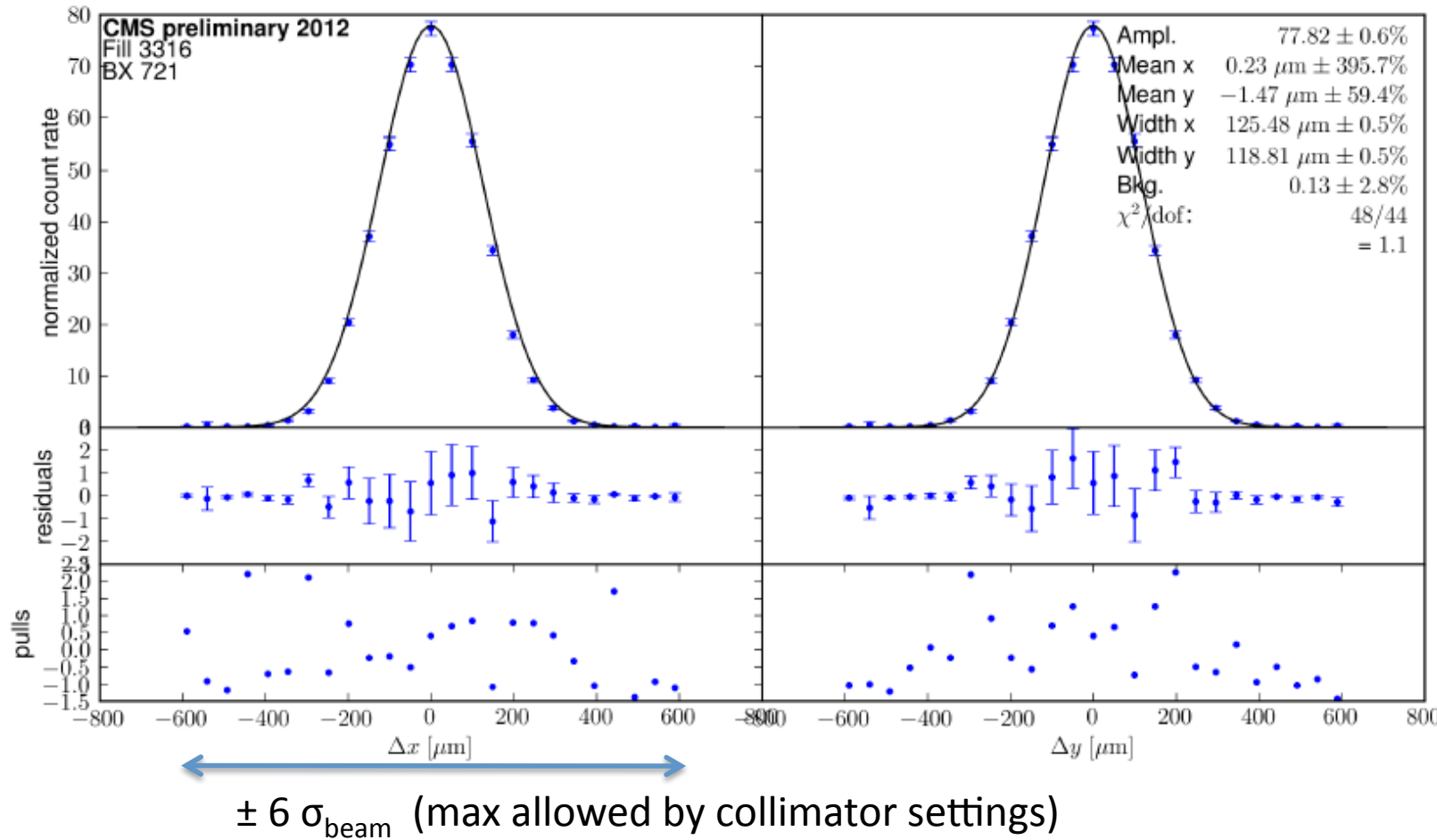
Use HFlumi as cross check

# VdM analysis, fill 3316

- Nov 2012 VdM scan campaign:
  - Dedicated LHC fill 3316 with  $\beta^*=11\text{m}$  (injection optics) zero crossing angle and 28 colliding bunches
  - 3 pairs of head on scans (X-Y, Y-X, X-Y) and 2 pairs of off-set scan ( $1\sigma$  and  $2\sigma$  separation in the orth. plane)
  - Consider only the 3 head-on scans for the calibration, offset scans were meant for possible X-Y correlations
- Analysis based on
  - Pixel cluster counting in AlCaLumiPixel stream in ZeroBias triggered data for 5 BX
  - HFlumi raw data (independent of CMS trigger), all 28 BX
- General ansatz:
  - Determine  $\sigma_{\text{vis}}$  from peak and width of the beam overlap shape for each BCID separately
  - Compute calibration from statistical average of the individual estimates
- X and Y scan beam overlap shape fit: Shown in the following
  - $(\text{Measured rate})/N_1 N_2$
  - where  $N_1, N_2$  are the beam currents
  - this corrects for the slight decrease in beam current during the scan; a per-mille effect on lumi

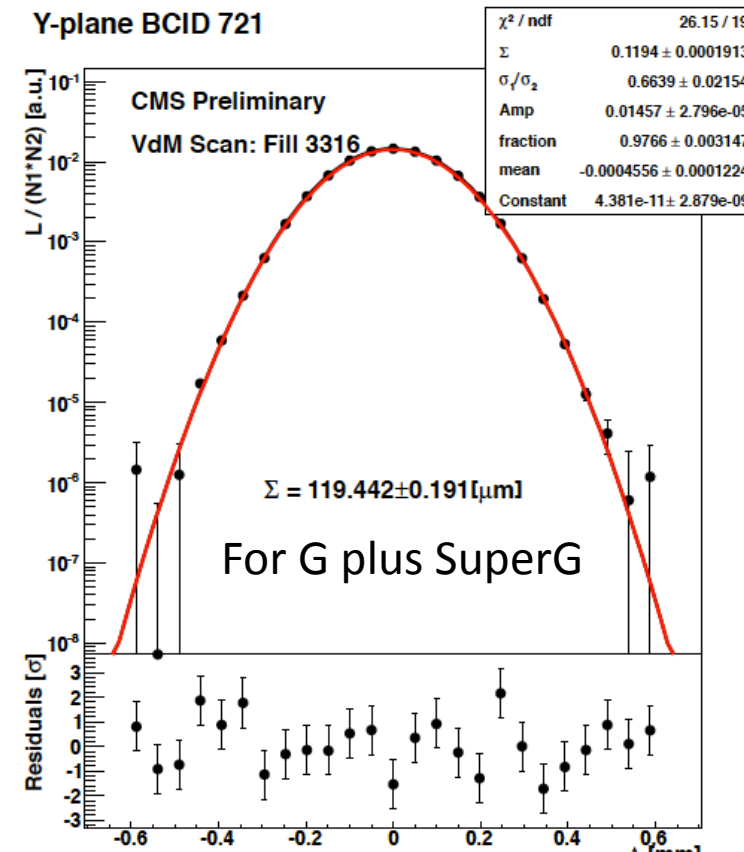
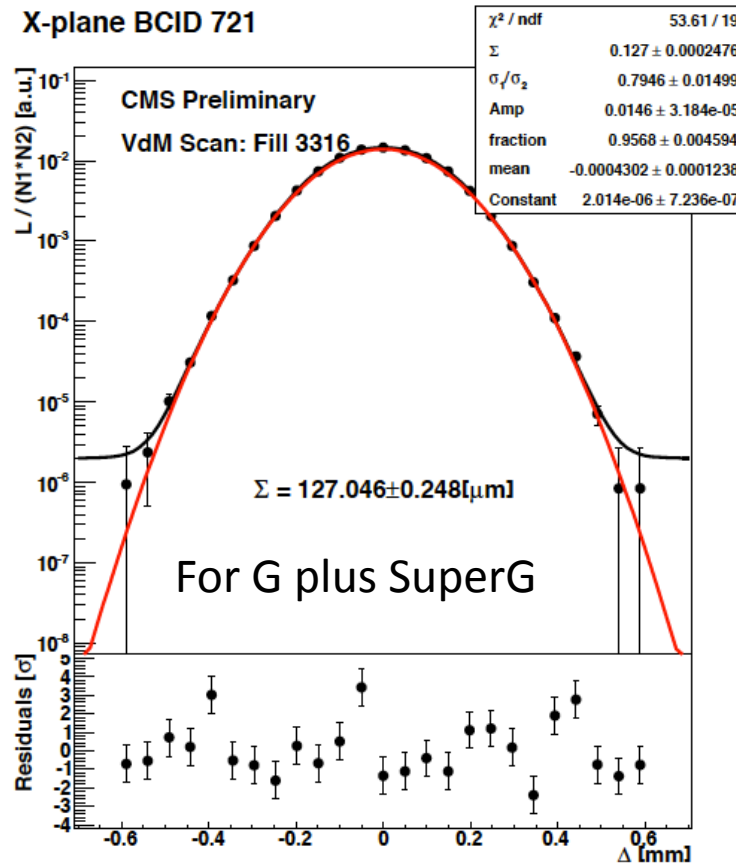


# Pixel cluster counting: Fit results



- Fit function is single Gaussian plus flat background
- In order to account for emittance growth (i.e. beam blow up during scan) correct fit result of X and of Y scan to intermediate point in time
- Fits have good quality, typical  $\chi^2/\text{ndof}$  around 1
- But statistically more limited than HFlumi

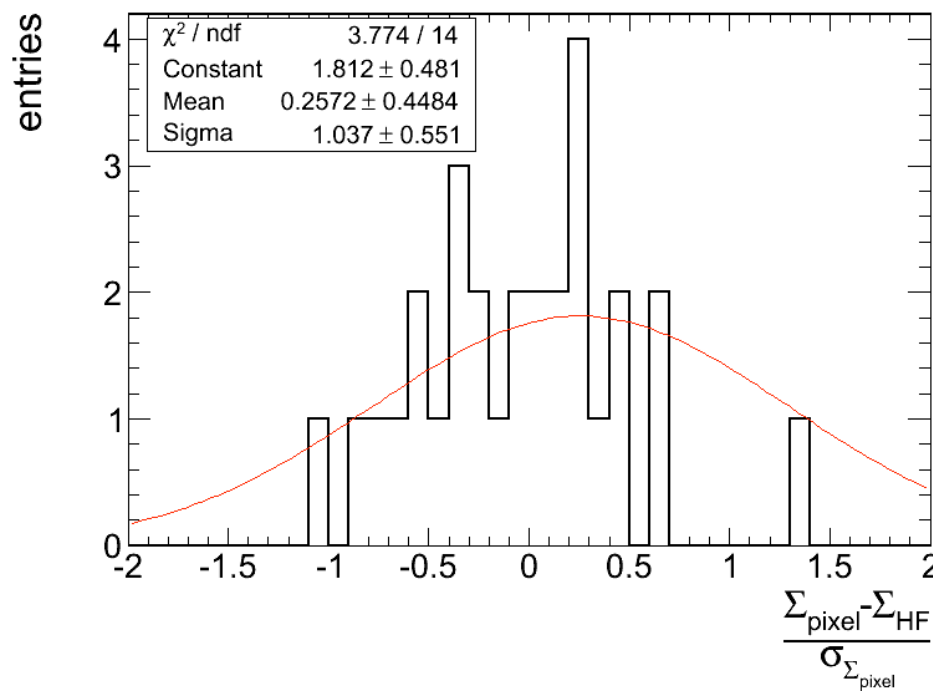
# HFlumi zero counting: Fit results



- HFlumi has larger statistical precision and hence was used to assess systematic effects from the choice of the fit function
- Functions tried:
  1. Single Gaussian plus flat background
  2. Double Gaussian, a. uncorrelated and b. correlated in X and Y , plus flat background
  3. Gaussian plus Supergaussian plus flat background, where Supergaussian means  $\exp(-0.5 [(x-x_0)/\sigma]^{2+N})$ , N=2; used in laser physics to describe higher order beam modes, with large kurtosis, i.e. more square than normal Gaussian; observed at SLC
- Little difference found between 1. and 2., while 3. generally resulted in  $\chi^2/\text{ndof}$  closer to 1

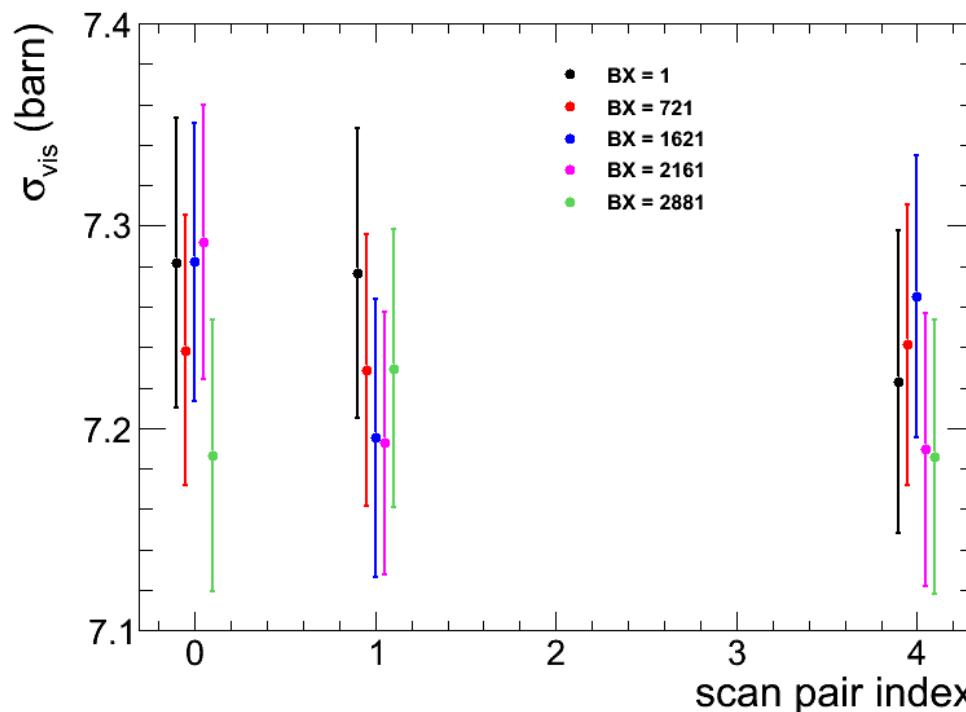
# Compatibility between pixel cluster and HFlumi zero counting fit results

- Look at the pool for each of the 5x3x2 shape fits (AlCaLumiPixel stream contains only 5 BCID, out of the 29 possible one)
- Compare results for Single Gaussian plus flat background fit
- Statistical uncertainty driven by pixel (0.5%)
- Excellent statistical compatibility



# $\sigma_{\text{vis}}$ results from pixel cluster counting

- No trends with time
- Per BX and per scan result very well compatible
- Overall statistical uncertainty  $\sim 0.5\%$
- Weighted average:  $7.230 \pm 0.038$  b
- Corresponds to a shift of the central luminosity value by a few per mil wrt previous preliminary calibration



See recently published PAS  
LUM-13-001

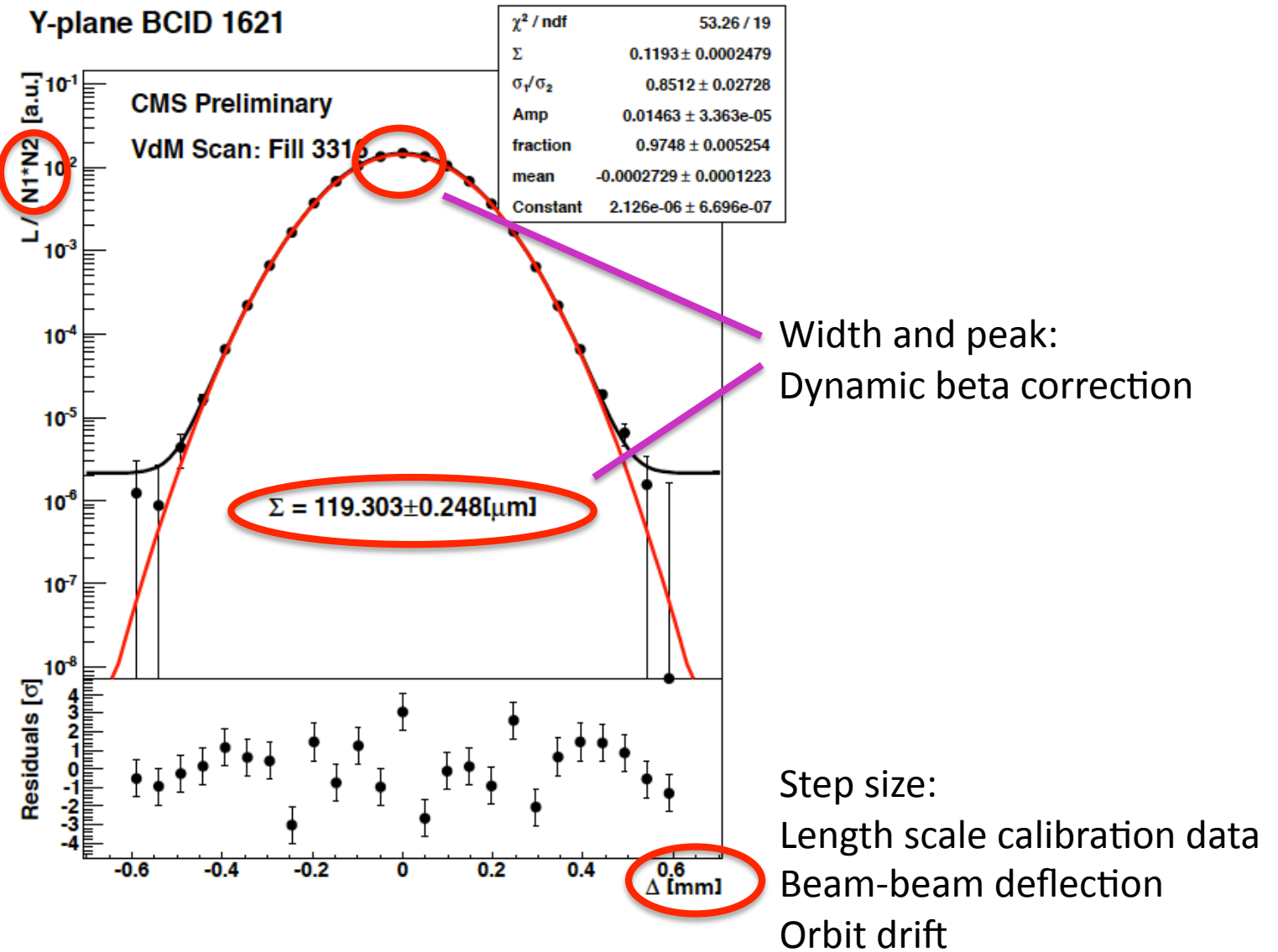
So far, so neat...

Now:

Corrections to VdM measurement

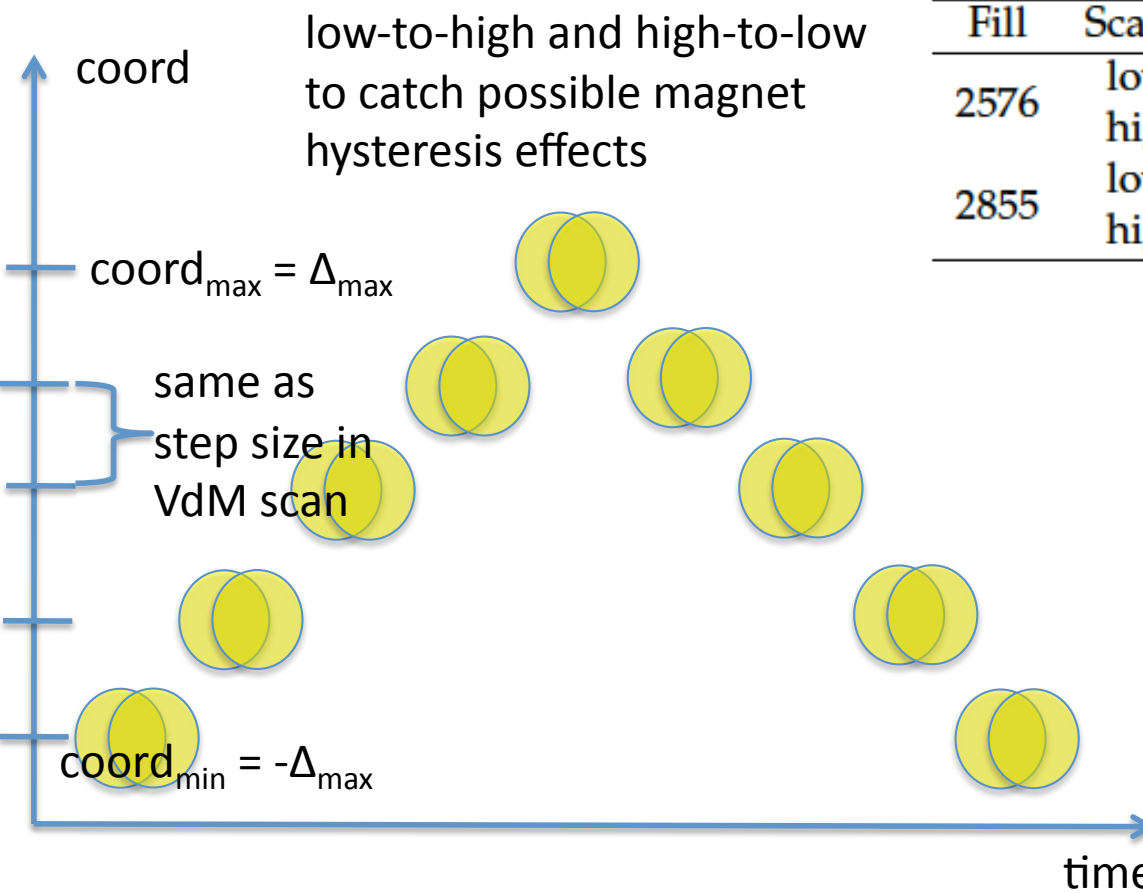
# VdM scans: Corrections

Currents:  
FBCT and DC-BCT  
Ghosts and Satellites

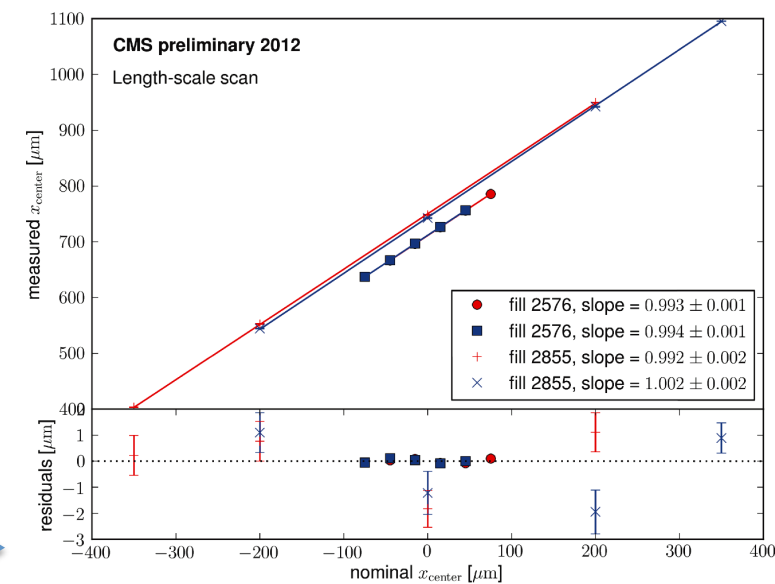


# Corrections: Length scale

- Actual beam separation during VdM scans given by LHC knobs, length scale calibrated with help of CMS primary vertex as measured for each nominal beam separation in a given scan
- Two length scale calibration data sets taken in 2012, fills 2576 and 2855
  - Use only 2855 since it was done with same optics as Nov VdM scans



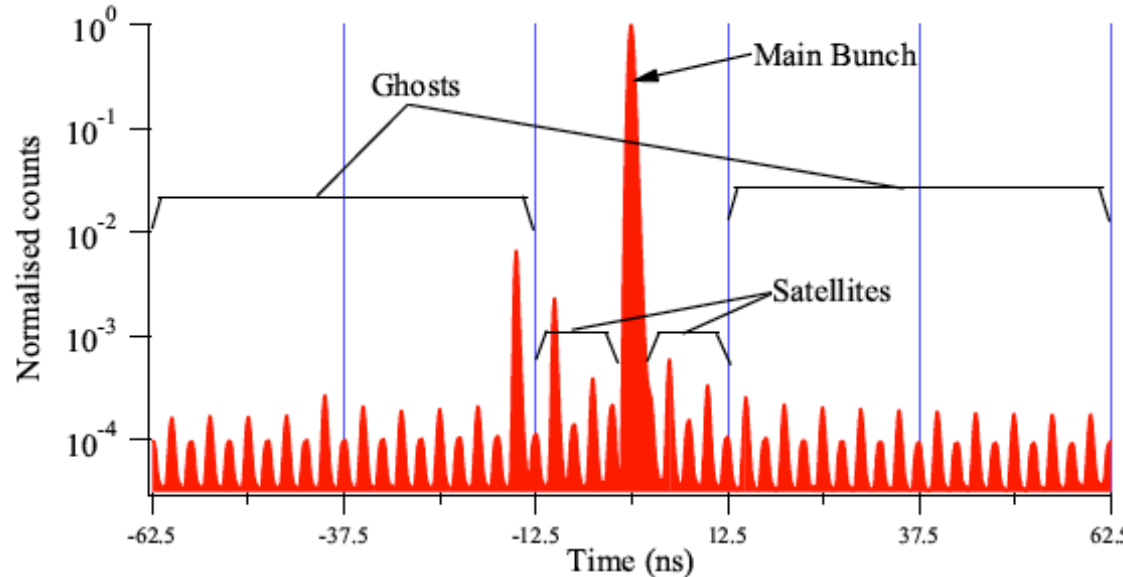
Fill	Scan direction	X-plane	Y-plane
2576	low-to-high	$0.993 \pm 0.001$	$0.994 \pm 0.001$
	high-to-low	$0.994 \pm 0.001$	$0.992 \pm 0.001$
2855	low-to-high	$1.002 \pm 0.002$	$0.993 \pm 0.002$
	high-to-low	$0.992 \pm 0.002$	$0.997 \pm 0.002$



# Ghosts and satellites in the LHC

BCNWG NOTE 4

CERN-ATS-Note-2012-029 PERF, June 12, 2012



- LHC operates at RF of 400 MHz
  - 35640 RF bins of 2.5 ns length, equidistantly distributed over ring circumference
- Nominally, only one out of 10 RF bins are filled with bunch
  - 3564 bunch slots or Bunch Crossing IDs (BCIDs)
- Ghosts:
  - Charge outside of BCIDs with nominally filled bunch
- Satellites:
  - Charge inside BCID with nominally filled bunch, but outside of that main bunch

Figure 1: Definition of ghosts and satellites (see text). Longitudinal profile taken with the LDM, in logarithmic scale.

- Ghosts and satellites can be measured by LDM (Longitudinal Density monitor – measures synchrotron light) or by LHCb (SMOG method – measures beam-gas interactions)
- Their intensity is typically down by  $10^{-4}$  compared to main bunch
- They may contribute to luminosity when running at zero crossing angle, as was done in the Nov 2012 VdM scans

# Corrections: Currents

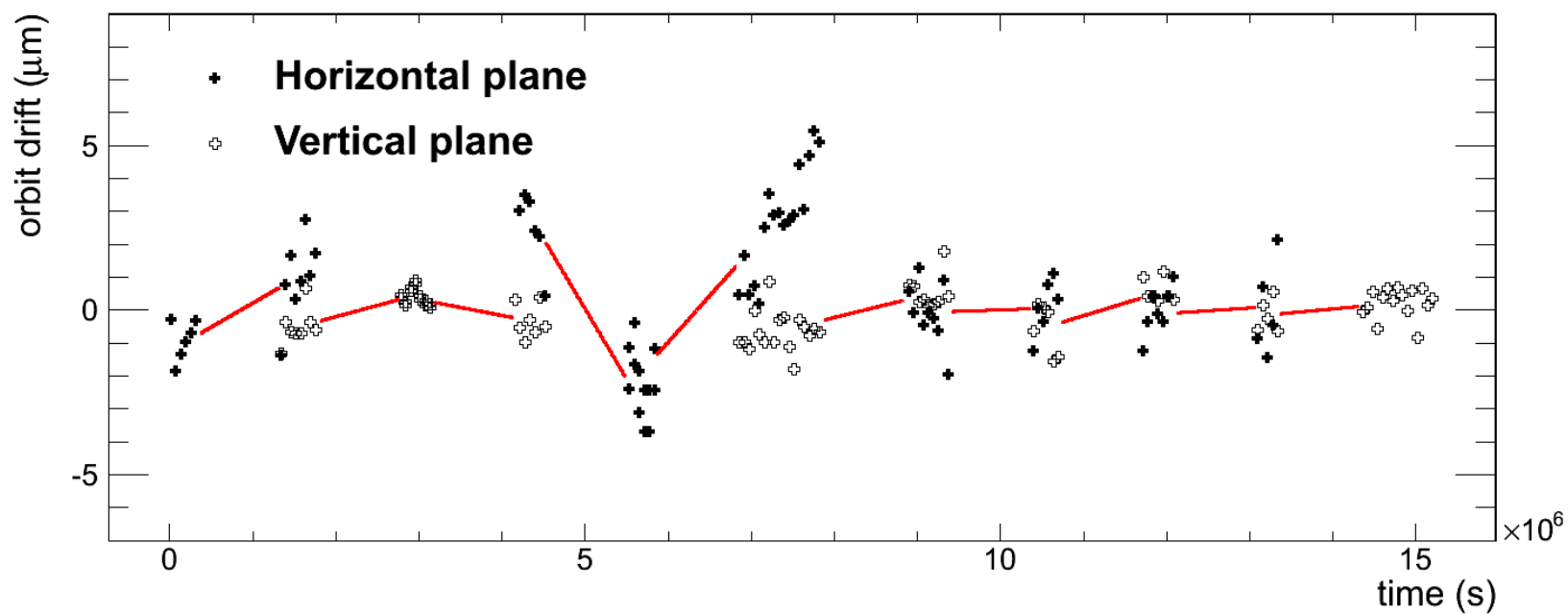
- Two beam intensity measurements , from DC-BCT and FBCT
- DC-BCT
  - Provides total intensity per beam, provides absolute value
  - Very precise, error per beam of O(0.2%) or O(0.34%) on product, but too slow for per-bunch measurement
- FBCT:
  - Provides, per bunch, intensity contained in bunch in question
  - Measures in 25 ns window, i.e. integrates over 10 RF bins of which only one is nominally filled
  - Calibrated such that `SumOverAllNominallyFilledBunches(FBCT)` = DC-BCT
    - This way FBCT is used only to determine what fraction of the total current was in which nominal bunch, while the total current is measured by DC-BCT
- For HFlumi: Need to correct for ghosts only, main-on-satellite interactions contribute to lumi measured by HF (integration time 25 ns)
- For pixel cluster counting: Need to correct for ghosts and satellites because main-on-satellite interactions have vertices displaced by at least 0.375 m and pixel barrel detector has a total length of just 56 cm
- Size of corrections from LDM and LHCb SMOG method:
  - For 3316 the ghost charge 0.2% in beam 1 and 0.06% in beam 2
  - Satellite charge correction ~0.08% in beam 1 and ~0.4% in beam 2

$$N^j(t) = \frac{N_{fast}^j(t)}{\sum_j N_{fast}^j(t)} N_{DC}(t)(1 - f_{ghost})$$

$$M^j(t) = N^j(t) \times (1 - f_{sat}^j)$$

# Corrections: Orbit drift

- During a scan the orbit can drift along the scan plan inducing a bias in the estimate of the beam overlap
- Beam POsirion Monitor (BPM) measurements (per beam, per CMS side) along the arcs are used to estimate the beam position at the IP
  - Measurement during the scan not reliable, linear extrapolation from before and after each scan
- Overall small effect (0.2%)



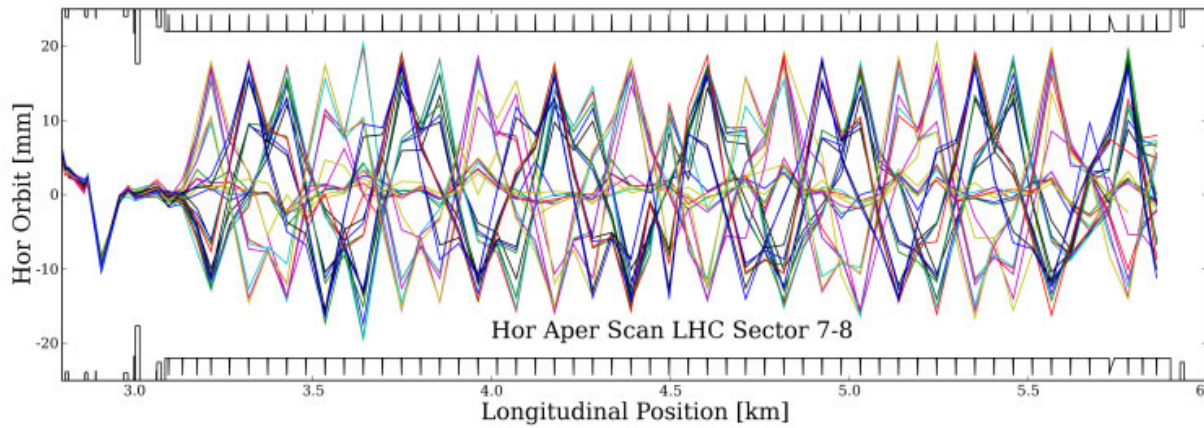
# Emittance and beta

$$\begin{aligned}
 L &= N_1 N_2 f n_b / A_{\text{eff}} \\
 &= N_1 N_2 f n_b / (4 \pi \sigma^2) \\
 &= N_1 N_2 f n_b / (4 \varepsilon \beta^*)
 \end{aligned}$$

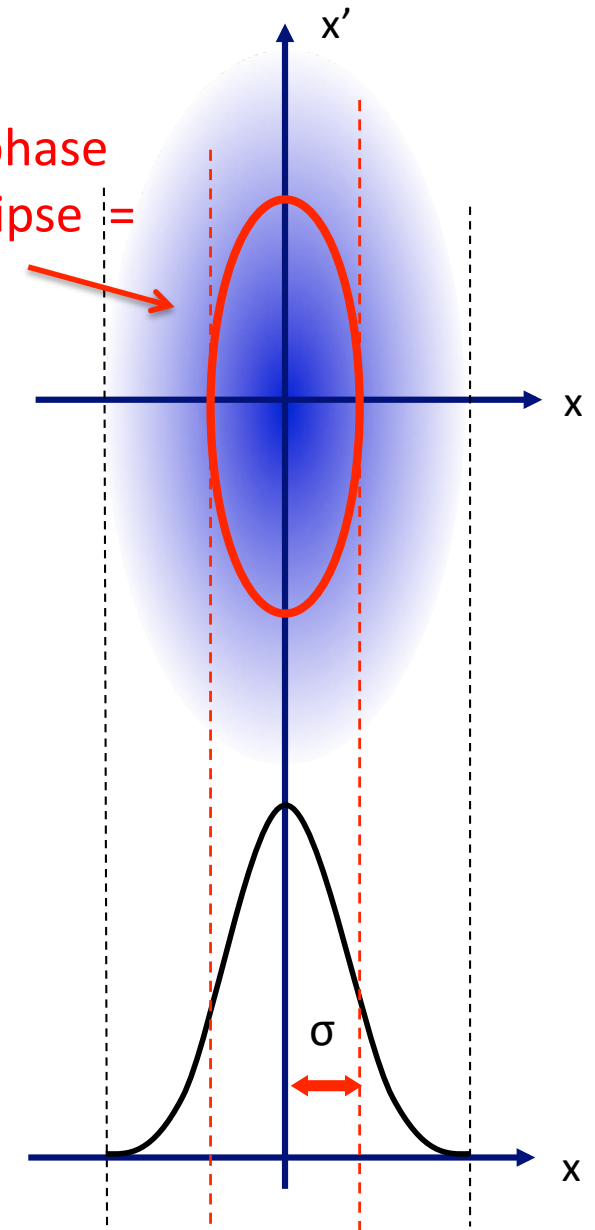
assuming round beams, i.e.  $\sigma_x = \sigma_y = \sigma$

$$\sigma = \sqrt{\text{Betafunction } \beta} \times \sqrt{\text{Emittance } \varepsilon}$$

magnet structure      particle ensemble

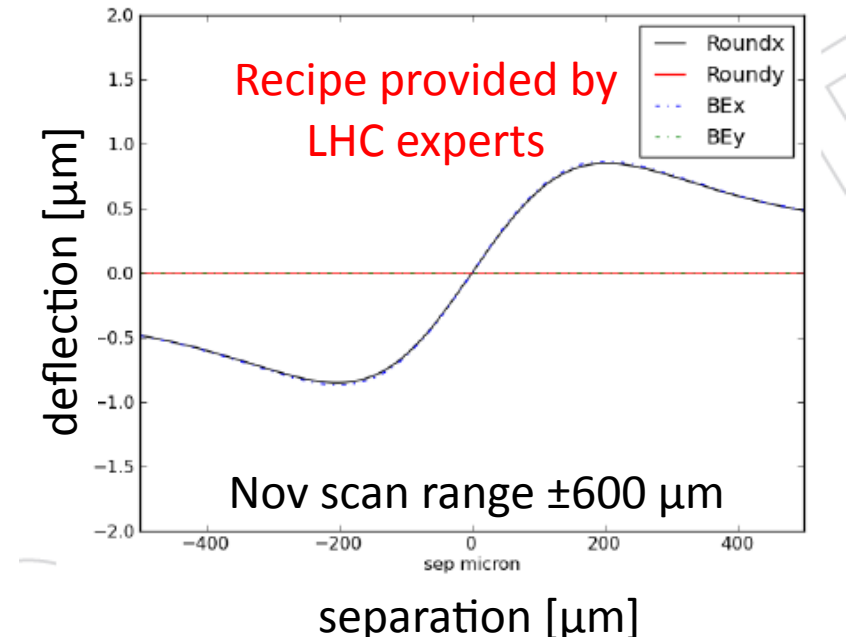


Area of phase space ellipse =  
 $\pi \varepsilon$



# Corrections: Beam-beam effects

- Electromagnetic interactions between crossing proton beams
- Dipolar kick (beam-beam deflection):
  - Repulsive force deflects the beams affecting nominal separation depending on the separation itself, the beam width and the current
  - Overall large correction, 1.5%
- Quadrupolar (de)focusing (dynamic  $\beta$ ):
  - Effective beam width modified depending on the separation
  - Peak luminosity (vertical shape of rate profiles) affected
  - Tricky effect, currently estimated to have small impact, (-)0.2%. We decided not to correct and assign large systematics
    - Correction was +0.8%, then fixed to -0.2%

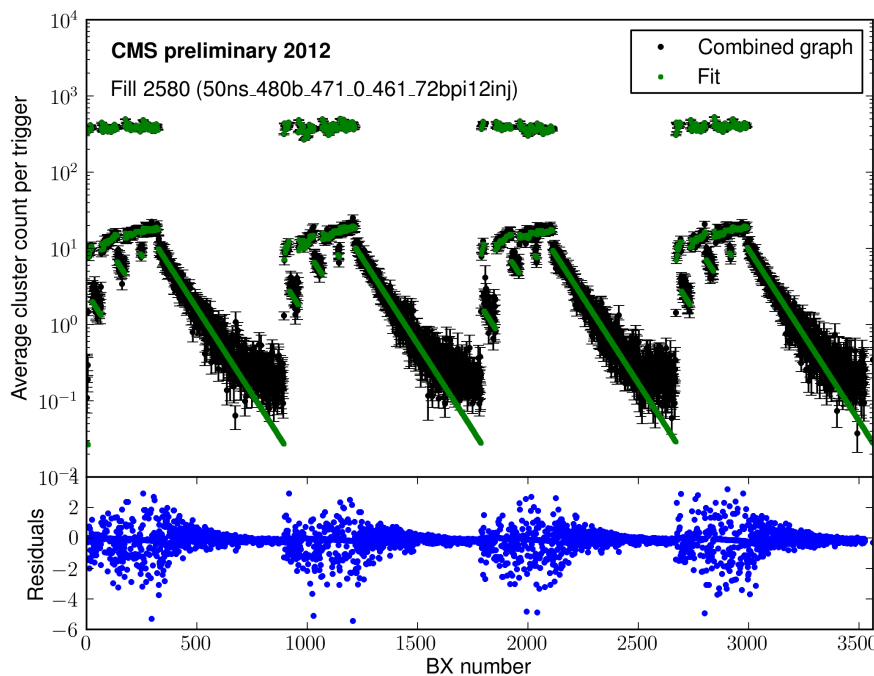


# Luminosity integration

- Assess effects from integration, i.e. from applying VdM calibration to full 2012 pp data set, for which pixel cluster counting result is used:
  - Pixel stability over 2012 run:
    - Select subset of pixel channels that make those ratios flat across the year, <<1% variation
  - Dynamic inefficiencies
    - due to high L1 rate, do not exceed 0.5%
  - Geometrical acceptance
    - possible effect due to length of luminous region ( $\sim 6$  cm long) found to be negligible
  - No instabilities vs pile-up observed
  - Afterglow gives 2% correction

# Lumi integration: Afterglow

- “Out of time response” featured by the cluster counting method:
  - Mild activation of the surrounding material
- Try to model and estimate the single bunch response assuming an exponential decay of the afterglow
  - Does not depend on the filling scheme
- Small contribution which however sums up to a non negligible component in highly populated filling schemes,  $\sim 2\%$  effect



Filling Scheme	Correction Factor
Multi_48b_35_3_6_4bpi14inj	$0.999 \pm 0.0\%$
Multi_52b_3_24_24_4bpi13inj	$1.000 \pm 0.0\%$
50ns_72_60_0_6_36bpi4inj	$0.992 \pm 0.1\%$
50ns_78b_72_0_48_36bpi3inj	$0.991 \pm 0.1\%$
50ns_84b_72_0_60_36bpi3inj	$0.991 \pm 0.1\%$
50ns_88b_75_0_60_36bpi4inj	$0.991 \pm 0.1\%$
50ns_264b_249_0_240_36bpi8inj	$0.990 \pm 0.1\%$
50ns_480b_471_0_461_72bpi12inj	$0.984 \pm 0.3\%$
50ns_624b_618_0_604_72bpi12inj	$0.983 \pm 0.3\%$
50ns_840b_801_0_804_108bpi13inj	$0.983 \pm 0.3\%$
50ns_840b_807_0_816_108bpi12inj	$0.983 \pm 0.3\%$
50ns_852b_807_0_816_108bpi13inj	$0.983 \pm 0.3\%$
50ns_1092b_1051_0_1032_108bpi12inj	$0.980 \pm 0.4\%$
50ns_1092b_1054_0_1032_108bpi12inj	$0.980 \pm 0.4\%$
50ns_1374_1368_0_1262_144bpi12inj	$0.977 \pm 0.5\%$
50ns_1374_1368_0_1262_144bpi12inj.V2	$0.977 \pm 0.5\%$
50ns_1380b_1331_0_1320_144bpi12inj	$0.977 \pm 0.5\%$
50ns_1380b_1377_0_1274_144bpi12inj	$0.977 \pm 0.5\%$
50ns_1380b_1380_0_1274_144bpi12inj	$0.977 \pm 0.5\%$

# Systematic uncertainties

# Systematics: Fit Model

- Fit function cannot be analytically predicted, we can toss a few reasonable guesses based on variation to gaussians
- No a priori good reason for which different luminometers should measure different shapes
  - But HFlumi has higher statistical precision
- Use HF measured shapes to study the effect of difference beam shape assumptions

$s_{vis}$ variation	Single Gaus	Double Gaus	Super Gaus
Scan 1	0.04%	0.04%	1.2%
Scan 2	-0.6%	-0.6%	0.6%
Scan 3	0	0	1.3%

- Gauss plus SuperGauss gives better chi2/ndf values
- Want to be conservative here, assume 2%
- For the future: Develop a VdM MC that can be tuned to describe both beam overlap shapes and beam spot position and width data, use for study of fit model bias

# Summary of corrections and uncertainties

- Main guideline: be conservative!, experience taught us that it is difficult to get all the unknowns under control

	Systematic	correction (%)	uncertainty (%)
Integration	Stability	-	1
	Dynamic inefficiencies	-	0.5
	Afterglow	~ 2	0.5
	Geometrical acceptance	-	0.3
Normalization	Fit model	-	2
	Beam current calibration	-	0.3
	Ghosts and satellites	-0.4	0.2
	Length scale	-0.9	0.5
	Emittance growth	-0.1	0.2
	Orbit Drift	0.2	0.1
	Beam-beam	1.5	0.5
	Dynamic- $\beta$	-	0.5
	Total		2.5

# Summary

- At CMS, we have in place a reasonably stable system with good redundancies for online luminosity monitoring
  - primarily based on HF empty tower counting
- Absolute luminosity calibration at the LHC requires dedicated special Van-der-Meer scans
- Analysis of these VdM scans is technically involved and requires a concerted effort of the experiments together with the machine
- Based on the November VdM scan campaign, where machine delivered very clean Gaussian beams, CMS derived an absolute calibration with the pixel cluster counting method with an overall uncertainty of **2.6%** (2.5% (syst), 0.5% (stat))
- We have ample VdM scan data in hand for detailed studies of further method uncertainties and systematics
  - non-factorization effects
  - non-Gaussian beams
- Understanding those is important since it is not guaranteed that the machine after LS1 will be able to deliver VdM scans of the same quality as the Nov ones
  - develop VdM scan Monte Carlo simulation that makes use not only of the beam overlap shapes during the scans, but also of beam spot position and width information

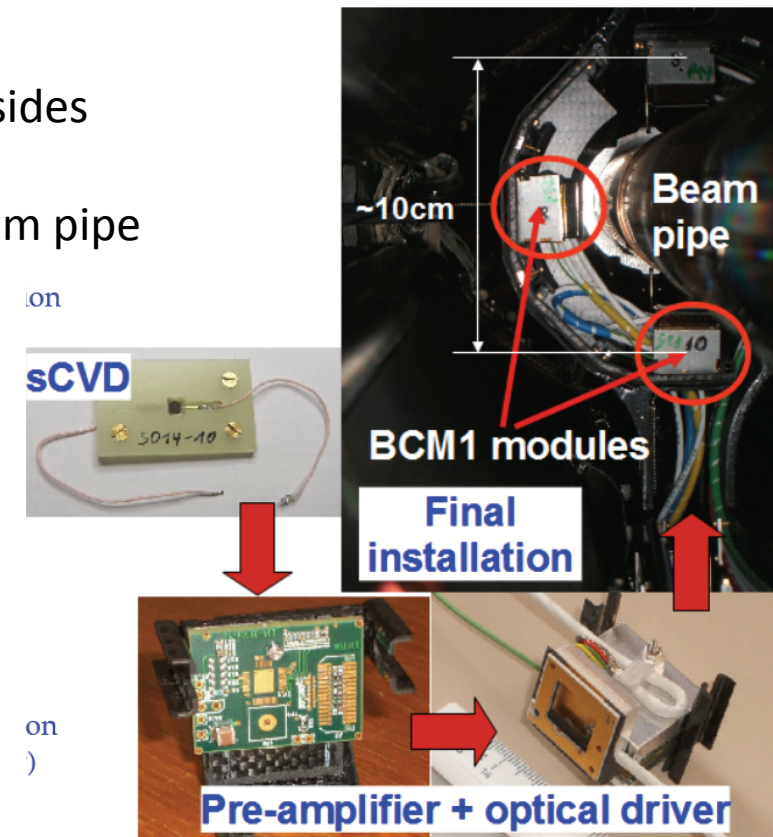
# Outlook: LS1 and after

- After LS1, will still have HFlumi as online method and pixel cluster counting as primarily offline method
- After LS1, will have additional luminometers: BCM1F and PLT

BCM1F: Fast Beam Condition Monitor ( $\sim 1$  ns)

- Single crystal diamond sensors metalized on both sides
- operated as solid state ionization chambers
- installed  $\sim 175$  cm away from the IP along the beam pipe
- High precision bunch-by-bunch luminosity

- LS1: Improved BCM1F readout electronics
  - In 2012, was calibrated to HFlumi after each run to compensate for gain losses in optical chain and rad damage to diamonds
  - Used primarily to ensure proper functioning of HFlumi and as failover

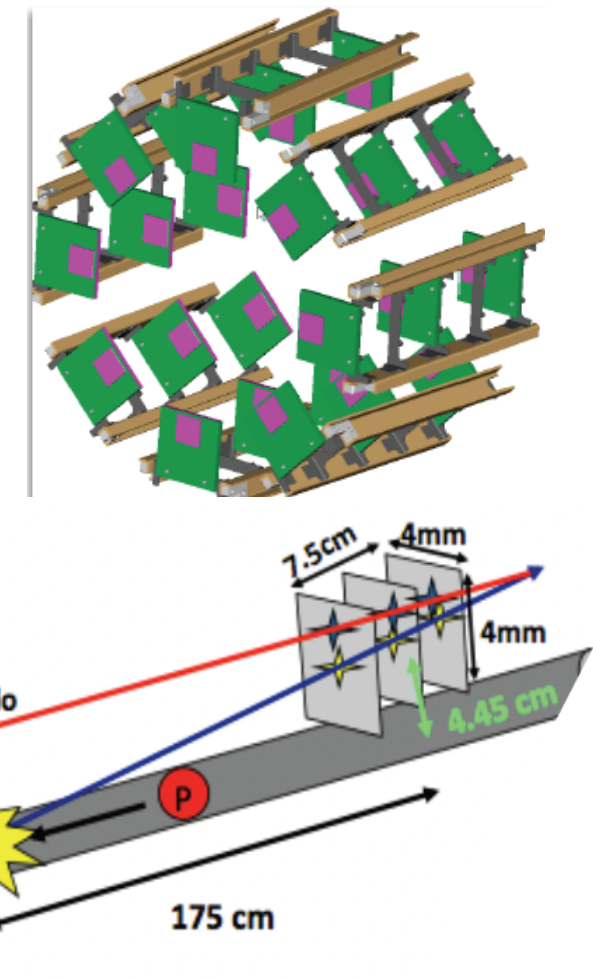


# Outlook: LS1 and after (II)

- After LS1, will still have HFlumi as online method and pixel cluster counting as primarily offline method
- After LS1, will have additional luminometers: BCM1F and PLT

## Pixel Luminosity Telescope

- High precision bunch-by-bunch luminosity
- Array of 3-plane telescopes each end of CMS
- Measure bunch-by-bunch 3-fold coincidence rate
- Pixel readout for tracking and diagnostics



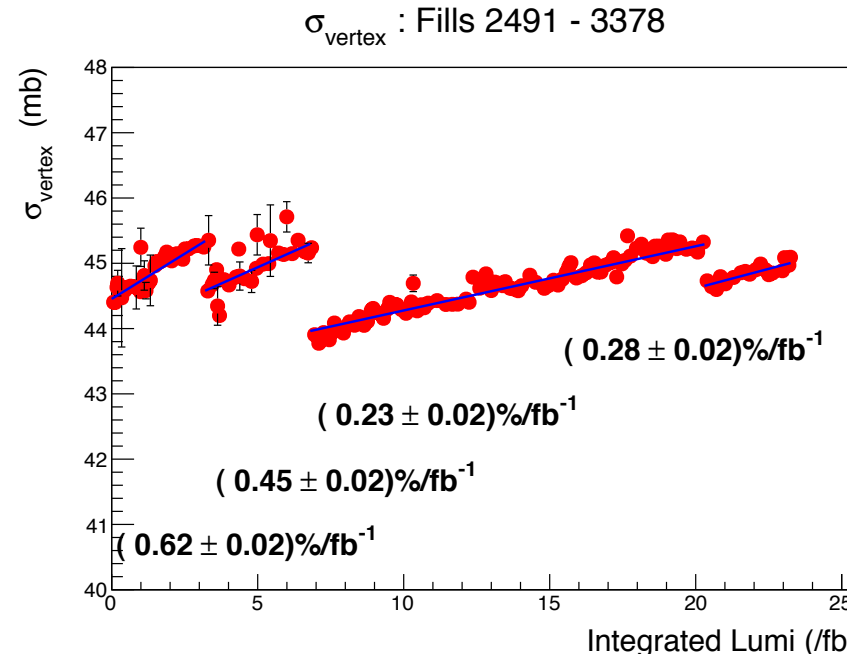
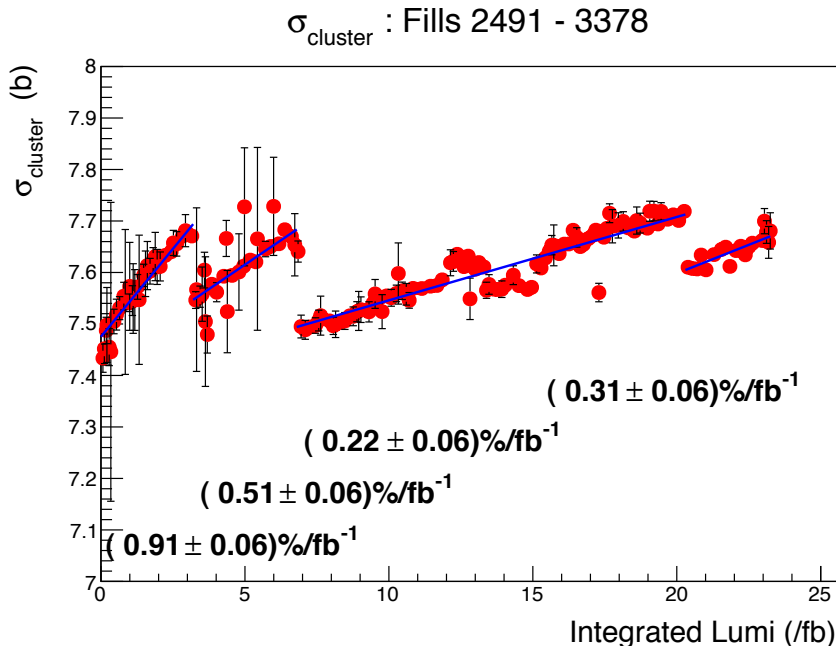
- LS1: Pixel-Telescope PLT will come on-line
  - Recent decision to switch from diamonds to Silicon (better understood behaviour in presence of rad damage)
  - Necessary installation of extra cooling line already completed

# Backup

# Online luminosity monitoring

- HFlumi
- BCM1F
- Pixel lumi
- DT

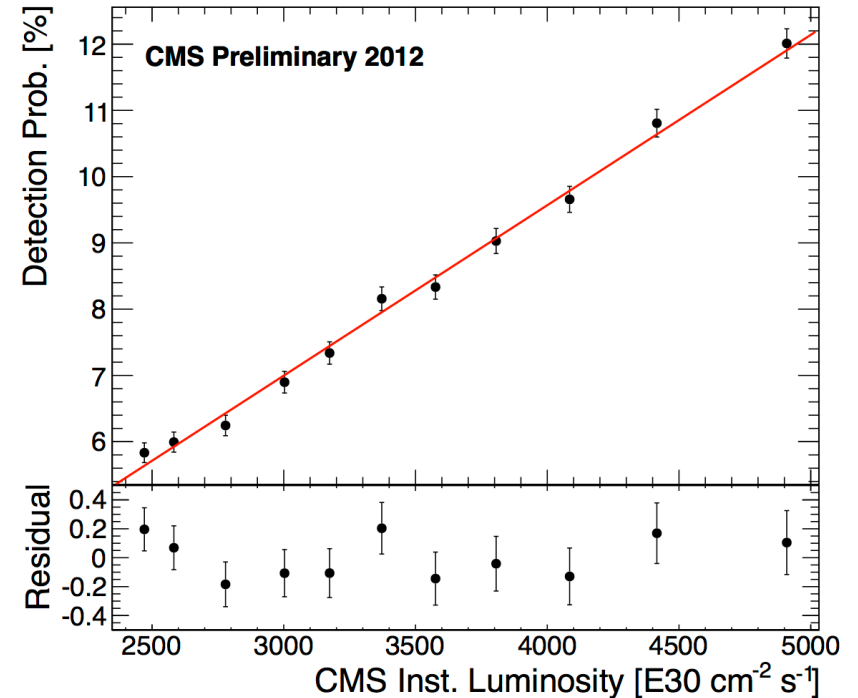
# HFlumi stability



- HFlumi calibration drift caused by HF response changes (gain deterioration, radiation damage)
- Drift monitored as fct of integrated luminosity with the help of pixel and vertex visible cross sections (see <https://twiki.cern.ch/twiki/pub/CMS/HFCalibrationMonitoring>)
  - Assume to first order that pixel cluster counting and vertex counting are stable over time
  - Use luminosity from HF to calculate visible cross sections from those counts
  - Changes in obtained visible cross sections then reflect changes in HF luminosity calibration
- HF gain recalibration done 4 times in 2012, clearly visible in plots
- Differences in pixel and vertex plots under investigation
- VdM scan results need to be corrected for these differences in HF response
  - Correction factors being worked on

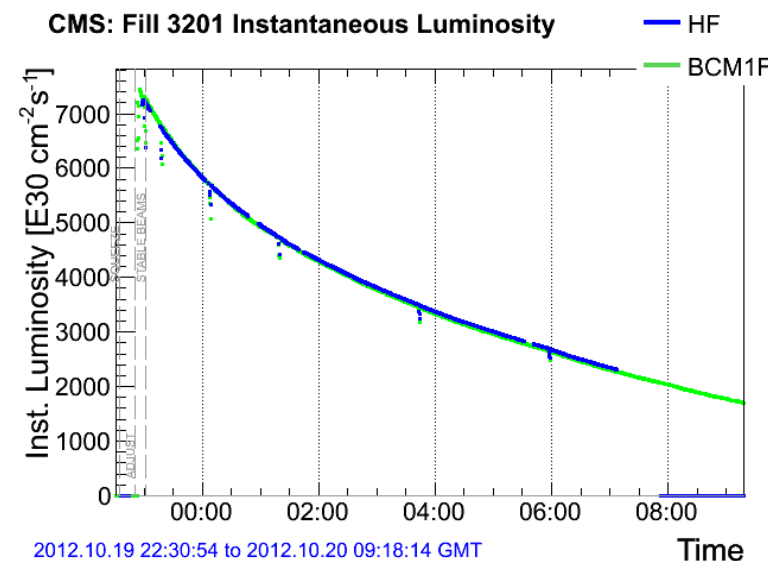
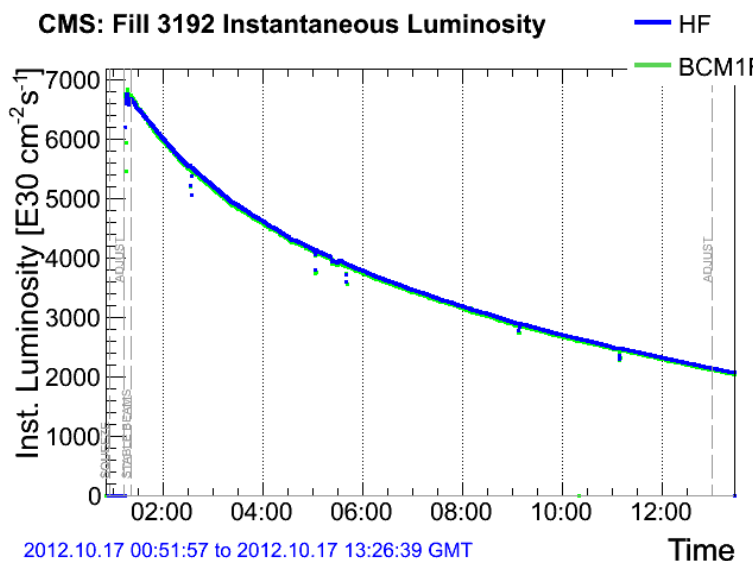
# BCM1F

- Single hit probability per bunch crossing for **1st** bunch in bunch train
  - Counting rate is reasonably insensitive to pileup during 2012
  - Use zero counting technique
- LS1 installation of additional channels, with smaller sensors will allow efficient measurement at higher luminosities (operation between LS1 and LS2)
  - Far from zero starving
- Demonstrated potential as online luminosity monitor during 2012



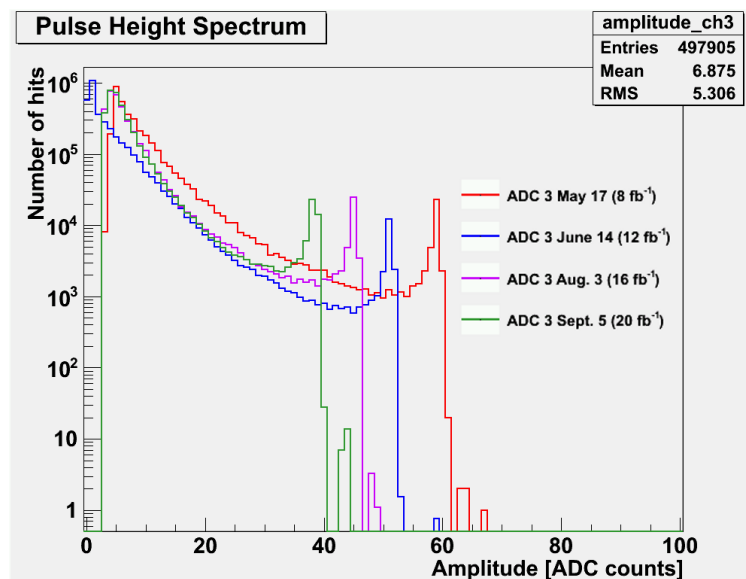
# BCM1F calibration

- Recalibrated to HF after every fill
- Most useful for
  - Confirm proper running of primary luminometer
  - Recovering delivered luminosity missing from the database
- Currently operates as failover for LHC publication if HFlumi glitch
  - dip/CMS/LHC/Luminosity shown on LHC page 1 will come HF
  - if HF is not updating (>30 sec) automatic switch to BCM (good to 0.1% because last 30 sec data used as scale factor before publishing to LHC)

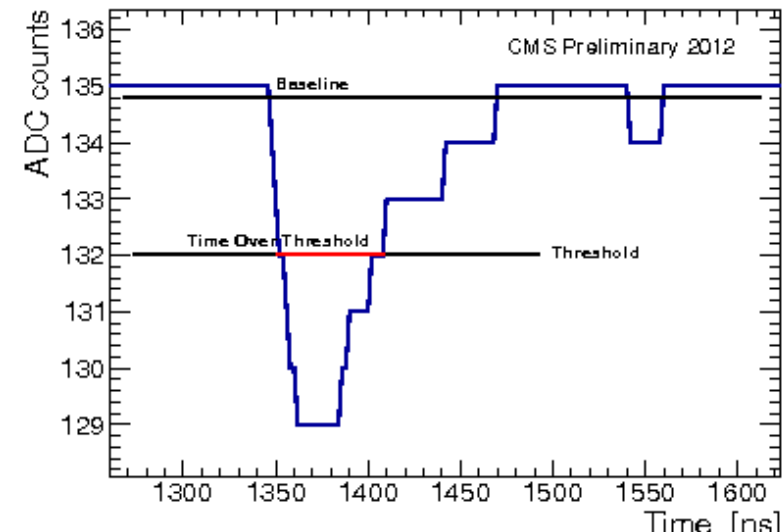


# BCM1F calibration/gains

- Recalibrated to HF after every fill to compensate for gain loss sources :
  - Gain loss measured in optical chain (laser driver)
  - Radiation damage seen in diamond sensors (loss MIP sensitivity in some sensors)
- For high rates; quadratic function is required.
  - Frontend preamplifier time resolution, peaking time 30 ns and limited dynamic range (will be upgraded in LS1)
  - Bunch-by-bunch dependent efficiencies



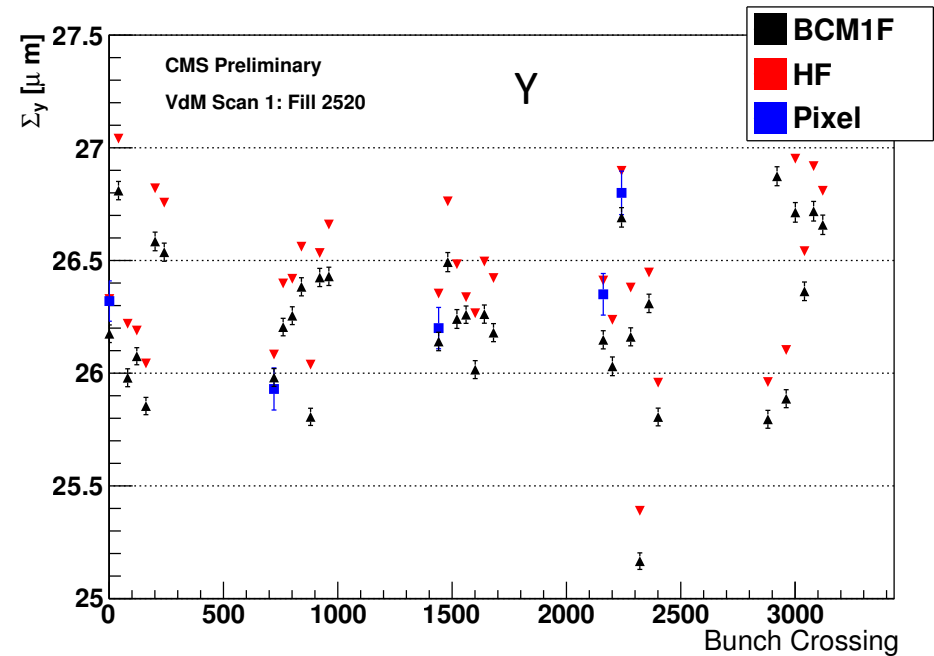
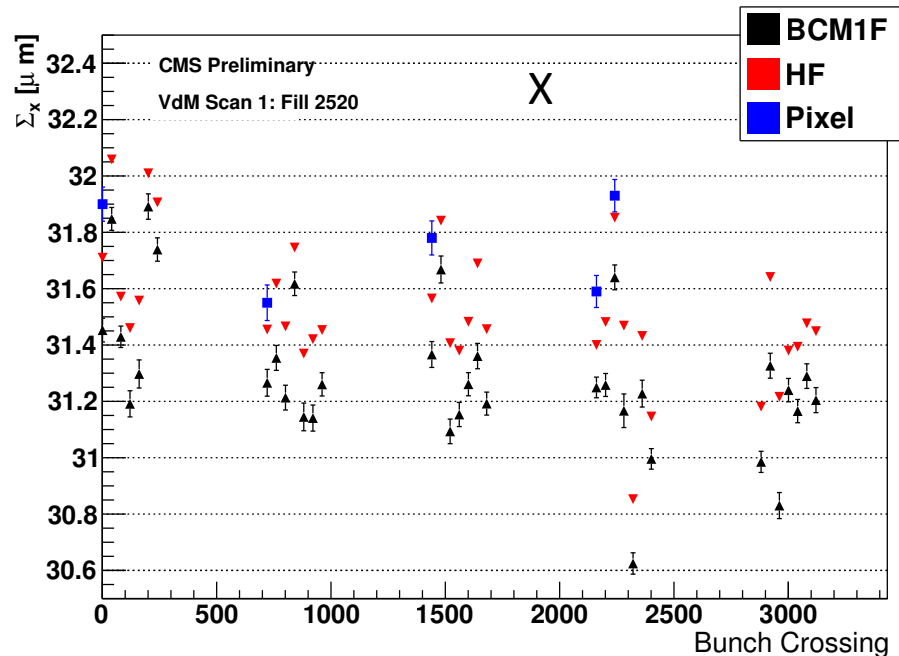
Loss in Gain



Addressing of systematics in LS1  
@ hardware level

# BCM1F consistency with other luminometers

- Example of April 2012 Fill 2520 VdM scan, agreement within 1% on average
  - All 8 diamonds in BCM1F used
  - 24 BCM1F diamonds foreseen after LS1 improving this cross-check functionality



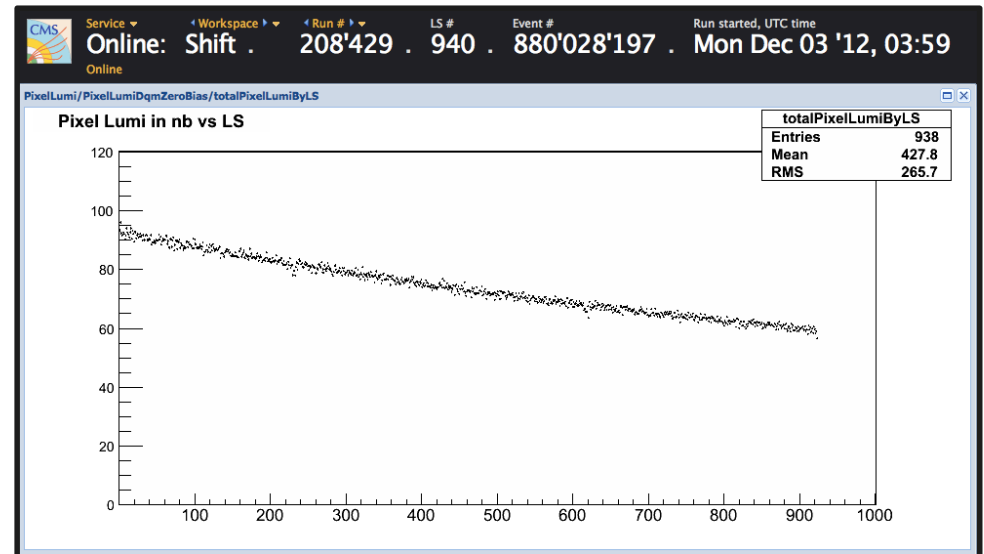
# BCM1F – systematics – LS1 actions

*2012 Running allowed us to identify various systematics to be addressed in LS1 in order to be a stand alone Bunch-by-bunch luminosity luminometer (more details Lisbon Lumi talk)*

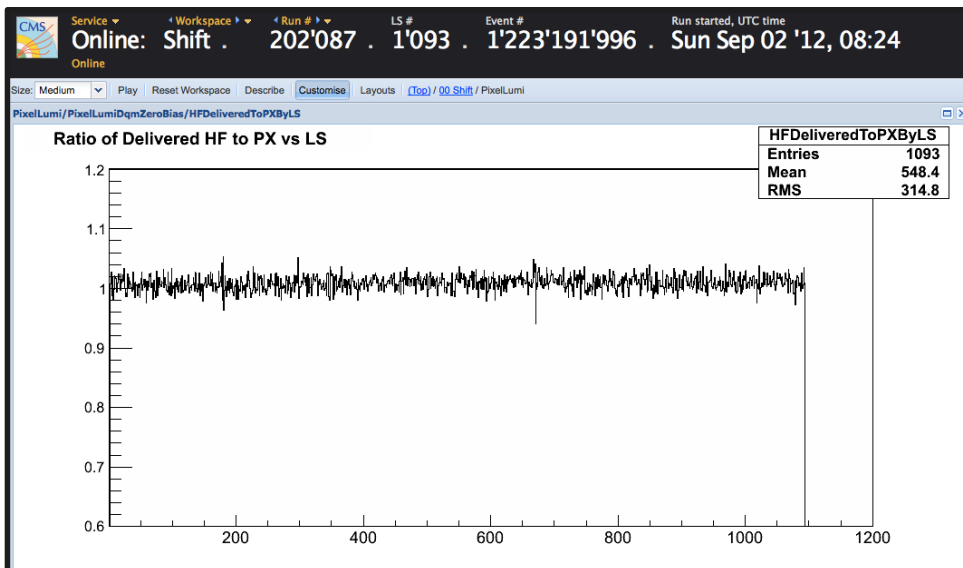
Systematic observation	Action LS1
Loss in optical gain ~ 35% radiation damage laser	Move Laser from R=4.5cm to R=12cm Automatic x2 gain test pulse monitoring in abort gap
Temperature dependence – optical transmission	Temperature monitoring (for feedback) <i>Ideally install cooling not baseline</i>
Loss MIP sensitivity – radiation damage full chain	X2.5 more gain (1-5 MIPs) in NEW ASIC frontend
HV and rate dependent gain - polarization	Operate high HV (1kV) Potential new surface treatment
Rate dependent efficiency, gain & pileup – frontend (peaking time + saturation)	NEW ASIC < 10 ns peaking time, fast recovery, non-linear gain for >8 mips Automatic x2 gain test pulse monitoring
Statistical sampling & granularity	8 diamonds (<2013) → 24 diamonds (potentially 48 channels). MC optimization ongoing. New diamonds, cabling, mechanics design and backend.

# Online pixel luminosity

- Application provides Pixel luminosity using the AlCaLumiPixel stream
  - Working quite well in Online DQM since July 26<sup>th</sup>, run 199739
  - Where to find it: WBM -> Online DQM GUI -> Workspace -> Shift -> PixelLumi

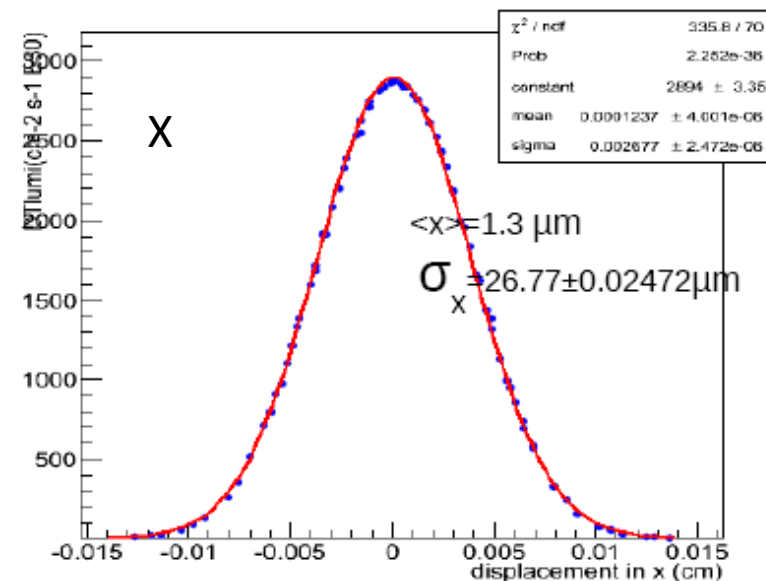
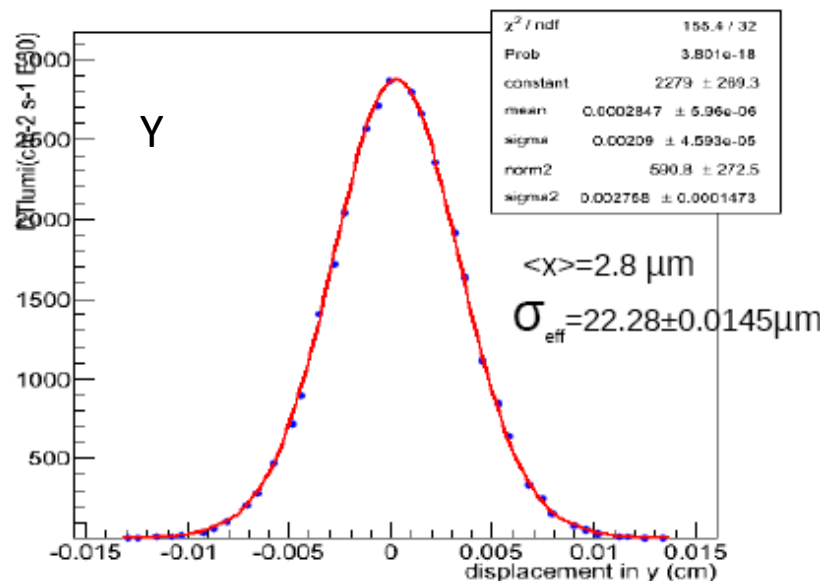


- Also provides the ratio of HF Lumi/ pixel Lumi (HF Lumi from DB)
  - Agreement is within 2%
  - A slight upward trend seen in very long runs: as lumi decreases so does PU, HF is less saturated, ratio decreases
- Also available in WBM



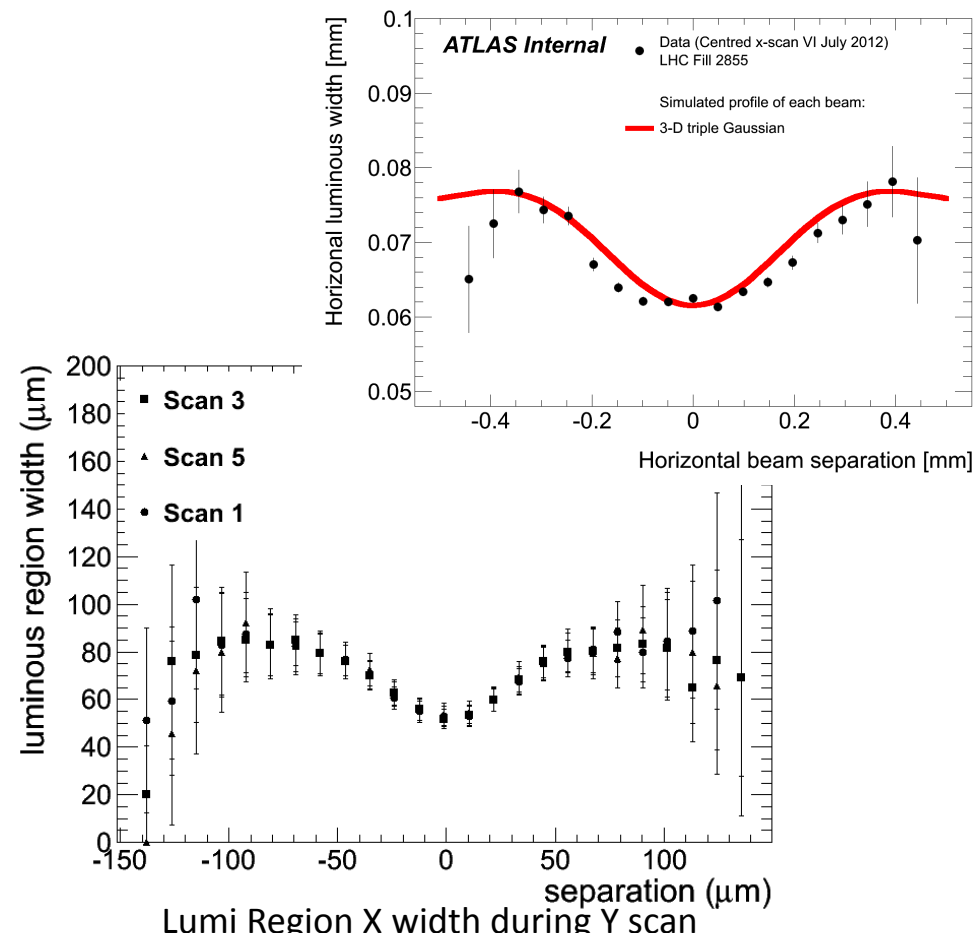
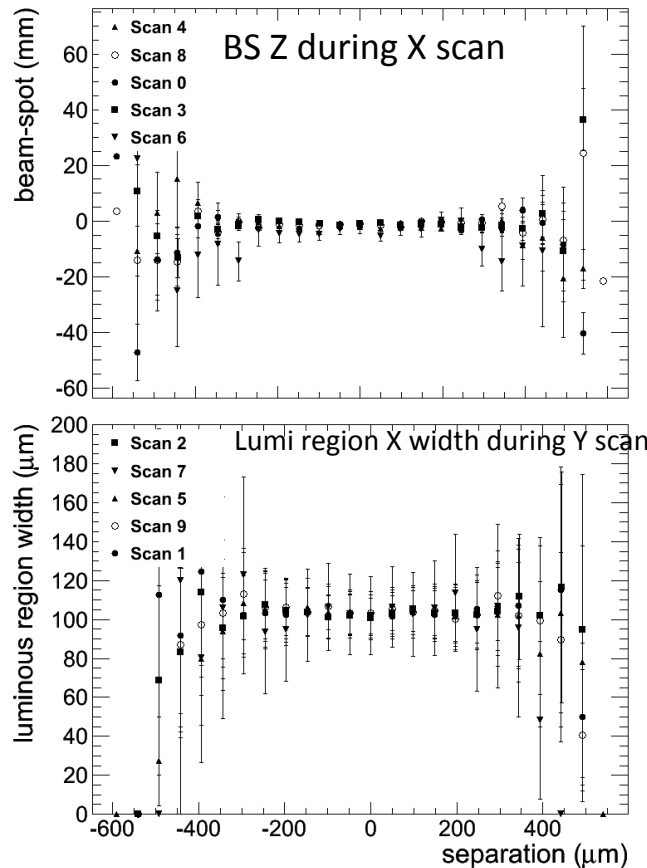
# DT barrel sorter rate luminosity

- DT Barrel sorter rate shows excellent correlation to HF and pixel lumis over several orders of magnitude
- Included in WBM, shown there with granularity of lumi section
- End-of-fill VdM scans of June used for calibration
- Study of lumi/bx for data from first half of 2012 shows that DT has, compared to HF, similar but opposite sign pileup dependence wrt pixel

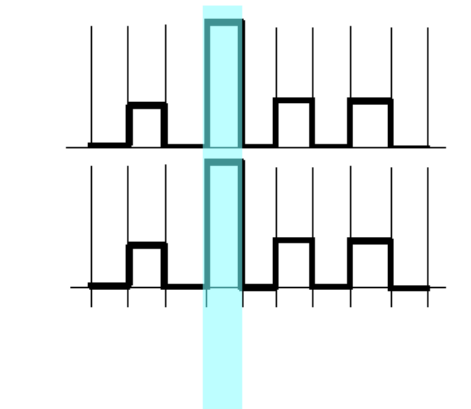


# Evidences from Luminous region

- If beams shapes are single gaussian and beams are crossing at null angle, the luminous region would not change during scan
- Separation dependent effects on the luminous region are indications of non trivial correlations



# Satellites



M-on-M: at IP, at time TM

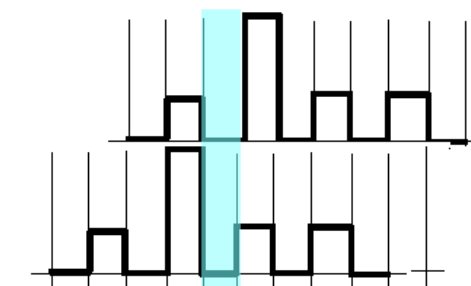
S-on-S: at IP plus/minus 0.75 ... 1.5 ... 2.25 ... m, at time TM, times 9

Interaction products from M-on-M reach HF at time T0:

M-on-M

S-on-S	-1.5 m	...	-0.75 m	...	IP	...	+0.75 m	...	+1.5 m
HF+	+5 ns	...	+2.5 ns	...	T0	...	-2.5 ns	...	-5 ns
HF-	-5 ns	...	-2.5 ns	...	T0	...	+2.5 ns	...	+5 ns

S-on-S interaction products will be seen by pixel barrel  
(~0.5 m overall length) only to very small degree



M-on-M: at IP, at time TM

M-on-S: at IP plus/minus 0.375 ... 0.75 ... 1.5 ... 2.25 ... m  
at time TM plus/minus 1.25 ... 2.5 ... 3.75 ... 5 ... ns

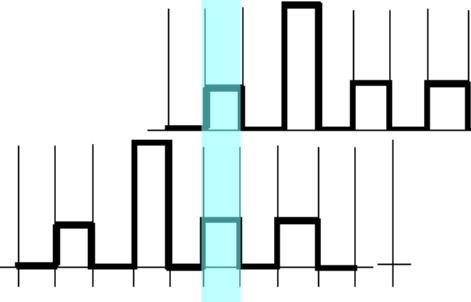
Interaction products from M-on-M reach HF at time T0:

Interaction products from M-on-S, created at time TM + n\*1.25 ns reach HF at time:

M-on-S	... -0.75 m	...	-0.375 m	...	IP	...	+0.375 m	...	+0.75 m	
HF+	...	+5 ns	...	+2.5 ns	...	T0	...	+0 ns	...	+0 ns
HF-	...	0 ns	...	+0 ns	...	T0	...	+2.5 ns	...	+5 ns

Interaction products from M-on-S, created at time TM - n\*1.25 ns reach HF at time:

M-on-S	... -0.75 m	...	-0.375 m	...	IP	...	+0.375 m	...	+0.75 m	
HF+	...	+0 ns	...	+0 ns	...	T0	...	-2.5 ns	...	-5 ns
HF-	...	-5 ns	...	-2.5 ns	...	T0	...	+0 ns	...	+0 ns

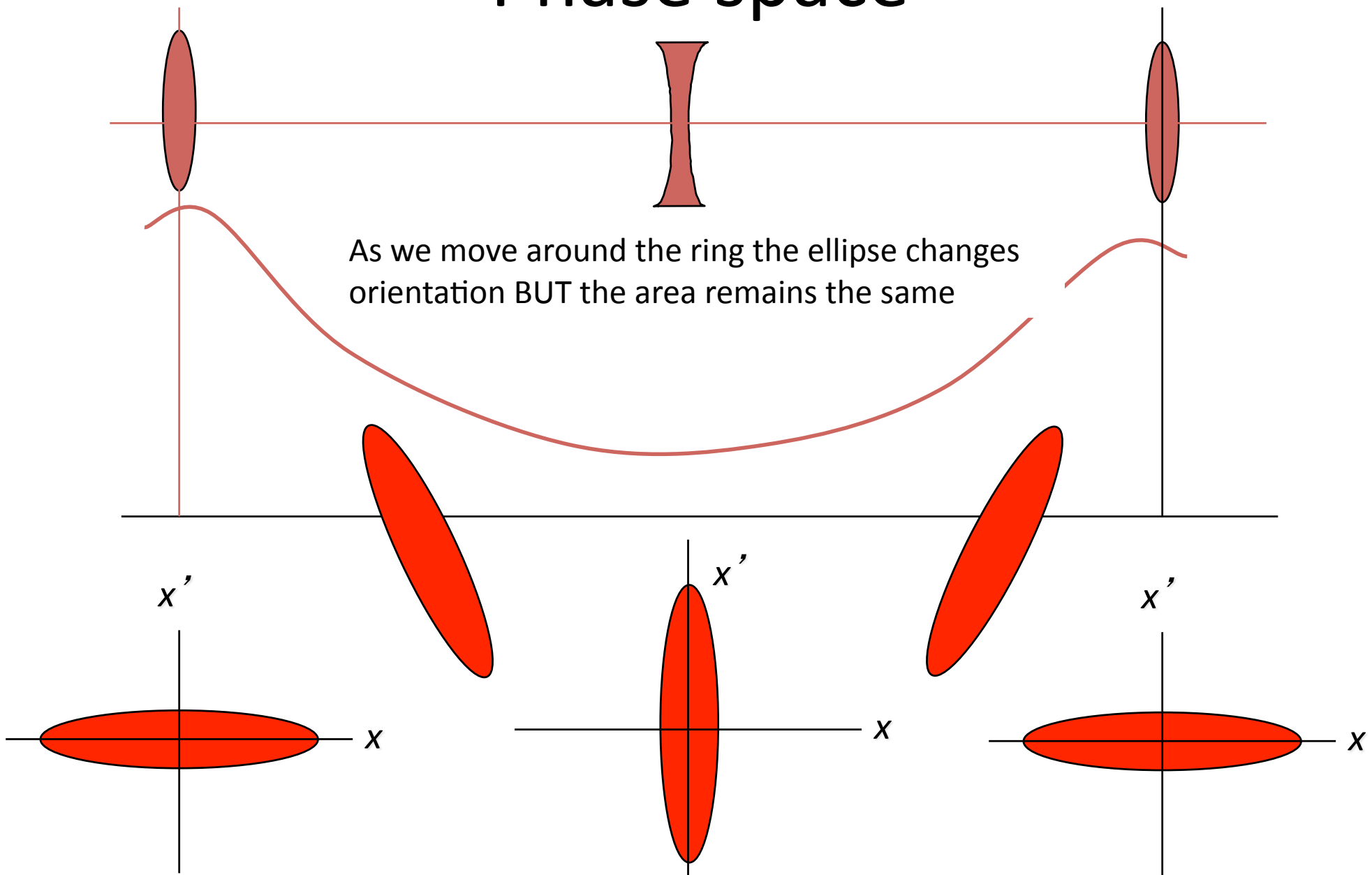


M-on-S interaction products from vertex closest to IP will be seen by pixel barrel  
(~0.5 m overall length) to some degree

# Currents: Instrumentation

- **LDM: Longitudinal Density Monitor**
  - Single-photon counting system measuring synchrotron light by means of an avalanche photodiode detector
  - The LDM is able to longitudinally profile the whole ring with a resolution close to the target of 50 ps.
  - The LHC is equipped with two sets of synchrotron light monitors, one for each beam, known as the BSRTs, located either side of the RF cavities at Point 4.
  - SR is emitted in a purpose-built undulator and in the D3 separation dipole immediately downstream.
  - Due to the small bending angle of the dipole, only 27 m downstream of the dipole are the SR and particle beams sufficiently separated to extract the synchrotron light. The SR is reflected downwards through a silica window onto an optical table where it is focused by two spherical mirrors. A beam splitter reflects approximately 7% of the available light onto the LDM detector.
- **BCT: Beam Current Transformer**
  - two DC current transformers (DC-BCT) and two fast beam current transformers (FBCT) per ring
  - Because of limited dynamic range, for pp provides usable measurement only for nominally filled bunches
  - They are installed in the long straight section in Point 4 of the LHC
  - Essentially circular magnets in which circulating charge passing through induces current
- **SMOG method in LHCb:**
  - individual beams “visible” in LHCb via interactions with residual gas
  - improve statistics by injecting neon into the LHCb IP region, improves BG from 0.1Hz/10<sup>11</sup> p to 20-40 Hz/10<sup>11</sup> p
  - allows to measure single beam shapes, position, angle, single bunch relative intensities, charge outside nominally filled bunches

# Phase space



# Corrections: emittance

$$\sigma_{vis} = \frac{2\pi A \langle n \rangle_{\Delta=0}}{N_1 N_2}$$

- The beam parameters (emittance and currents) change with time, we are measuring a moving target
- The elements in the formula defining the visible cross section need to be evaluated at a common time
  - Beam currents are monitored frequently, each rate measurements is normalized to the actual current values
  - The rate profiles amplitudes are fitted together (simultaneous fit of X and Y scan). They need to be corrected for
  - The width of the beams are different w.r.t when not probed
- Extrapolating rates and widths at the midpoint between the X and Y scan allow simplified treatment

# Corrections: emittance (2)

- Basic assumption: linear time dependency of all relevant quantities
- Emittance rate change estimated as the difference between Luminosity and Currents:

$$L(t) = L_0(1 + m_L t) = k \frac{N^2(t)}{\epsilon(t)} = k \frac{N_0^2(1 + m_{N^2} t)}{\epsilon_0(1 + m_\epsilon t)}$$

$$m_{N^2} - m_L = m_\epsilon$$

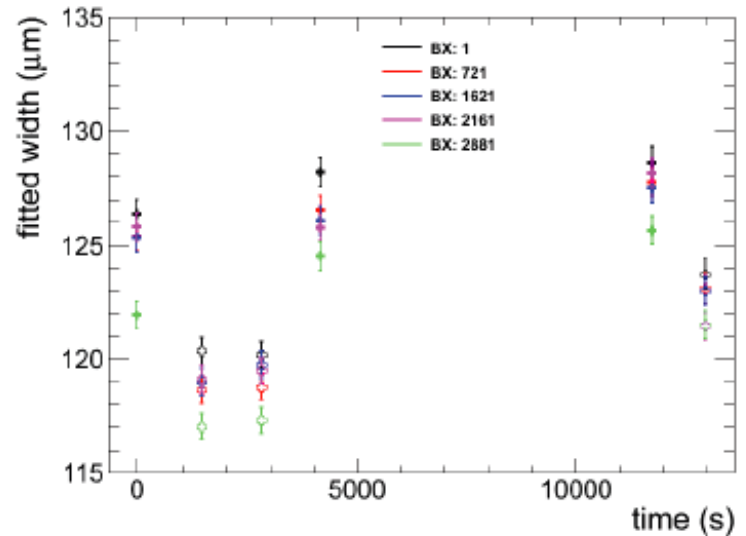
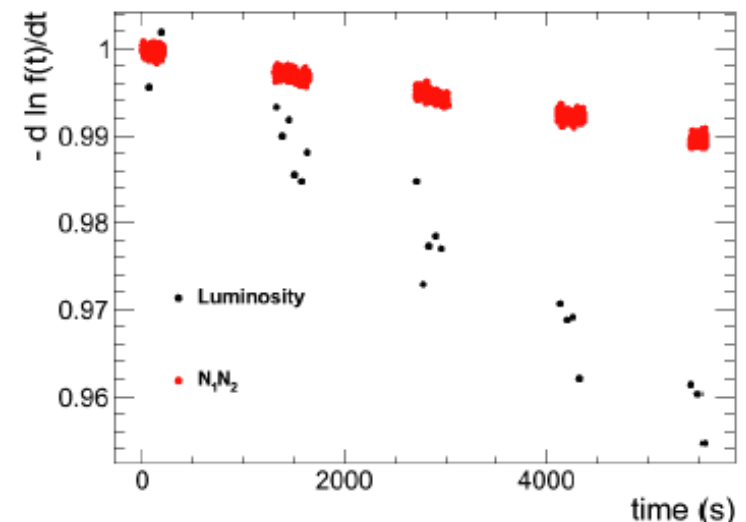
- Correction:  $1 \pm m_e D_t / 2$ ,  $m_e \sim 5 \text{e-}6/\text{s}$ ,  $D_t \sim 1500\text{s}$
- Hardly affect results, fit quality improves
- Widths measurements at  $\pm D_t / 2$  compensate:

- Bias proportional to difference of the Y and X growth rate

$$\Sigma_x(t_0)\Sigma_y(t_0) \rightarrow \Sigma_x(t_0 - \frac{\Delta t}{2})\Sigma_y(t_0 + \frac{\Delta t}{2})$$

$$\Sigma_{x,y}(t) = \Sigma_{0,x,y}(1 + m_{\Sigma_{x,y}} t) \rightarrow \frac{\delta(\sigma_{vis})}{\sigma_{vis}} \cong (m_{\Sigma_y} - m_{\Sigma_x}) \frac{\Delta t}{2}$$

- $m_s$  from width evolution in 3 scan pairs
  - $(m_{s_x} - m_{s_y}) \sim 5 \text{e-}7\text{s} \Rightarrow$  bias negligible



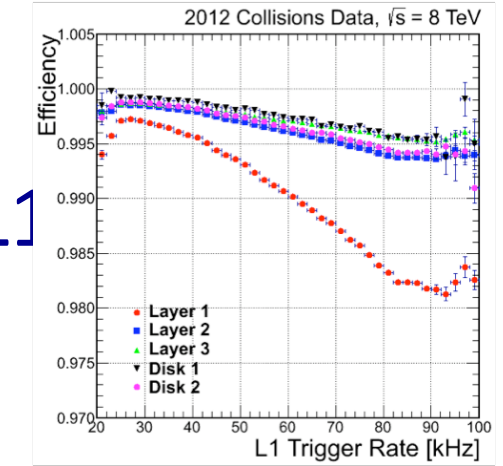
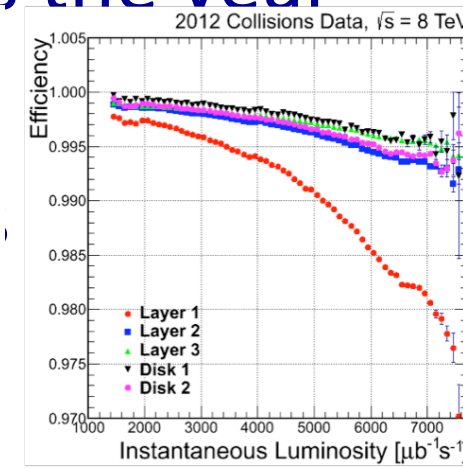
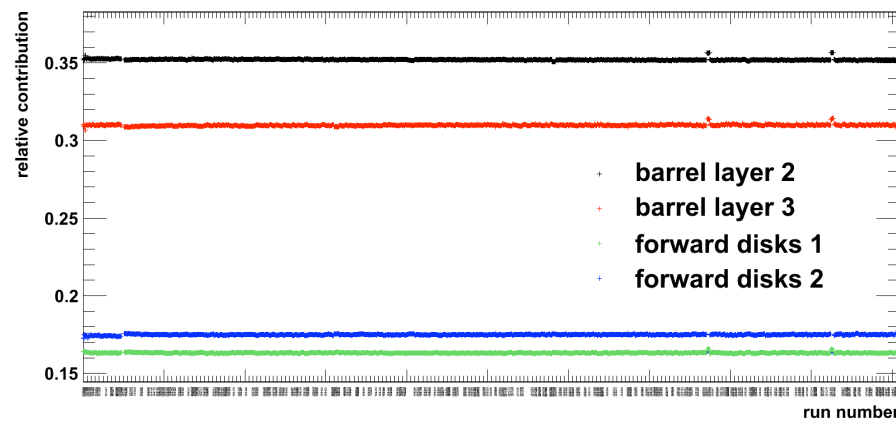
# Summary

## Corrections and systematics

- Wrt information provided by machine, sent to CMS via DIP
  - Currents
    - Measured by FBCT and DCCT
    - Need to be corrected for satellites and ghosts, which are determined with LDM and by LHCb (SMOG, BIG)
  - True step size:
    - Determined via special length scale data taking
- Wrt beam-beam effects inherent to LHC operation:
  - Beam-beam deflection
  - Dynamic beta correction
  - Orbit drift
- Wrt effects from integration, i.e. applying VdM calibration to full 2012 pp data set, for which pixel result is used:
  - Pixel stability over 2012 run
  - Afterglow
  - Dynamic inefficiencies
  - Geometrical acceptance

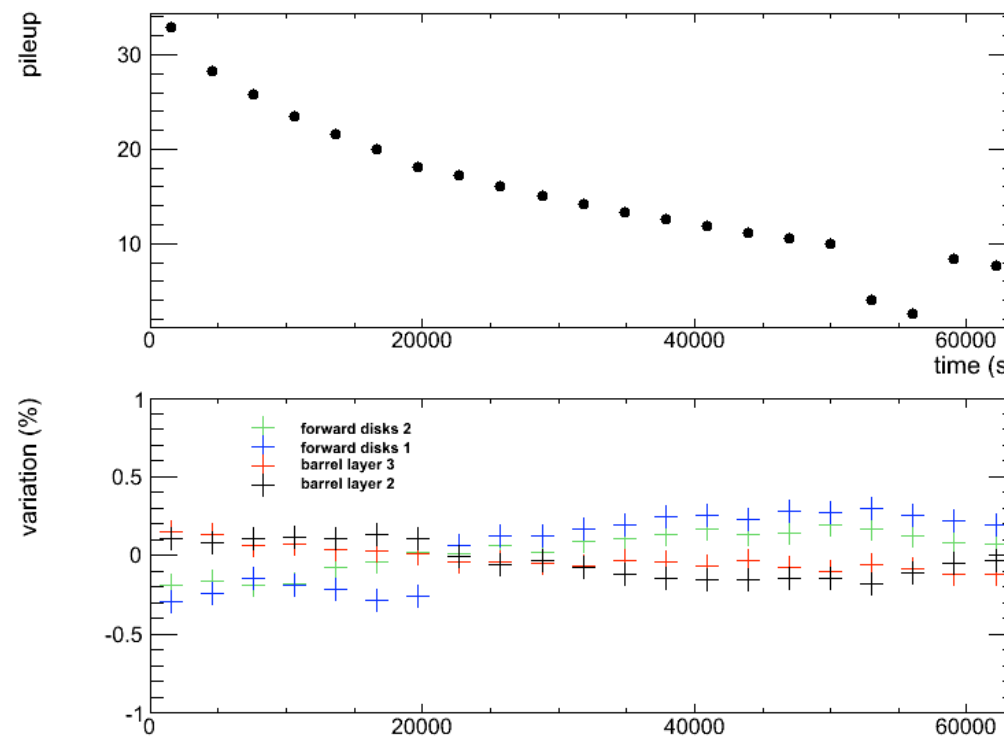
# Pixel cluster counting stability

- Several reasons to believe pixels are very stable
  - Other luminometers (e.g. HF) calibrated vs pixels
- Main figure of merit is the ratios of the pixel modules relative to the total cluster counting
- Select subset of pixel channels that make those ratios flat across the year



# Stability vs PU

- Consider fill 3236, very long, with a scan at the end
- Compare PU vs time with variation of the ratio vs time
- No app



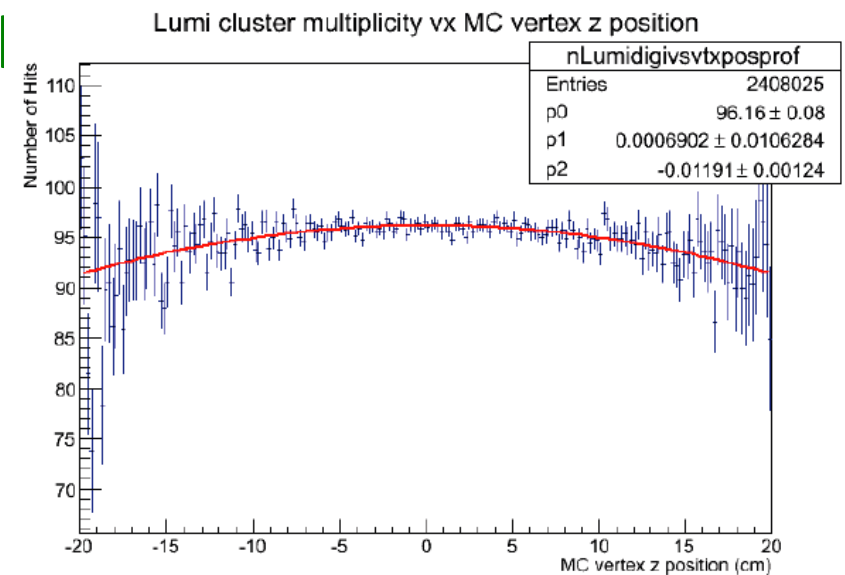
# BS and geometrical acceptance

- Luminous region  $\sim 6\text{cm}$  long, might have effect on the pixel detector acceptance
- Use MC to estimate effect:
  - Compute pixel hits vs z position of generated vertex

$$A(z) = \frac{a}{c}z^2 + 1 \rightarrow \int g(z)(1 - A(z))dz = \frac{a}{c} \int z^2 g(z)dz \sim \frac{\sigma_z^2 a}{c} \cdot (z)$$

~~... distribution, ... acceptance function ...~~

- With  $a=0.2, c=6\text{cm}$  > negligible effect (0.3%), not corrected for



# VdM Systematic uncertainties

- Length scale:
  - From comparison between measurements: 0.5%
- Currents:
  - DC-BCT scale: 0.3%
  - Ghost and satellites: 0.2% (50% of correction)
- Emittance growth:
  - 0.2% from emittance growth rate uncertainty
- Orbit correction:
  - Assumed 50% of the correction => 0.1%
- Beam-beam:
  - LHC experts suggest 20% uncertainty in their procedure, conservatively take 0.5%
- Dynamic beta:
  - 0.5%, twice the would-be correction or half of the latest fix

# Integration systematics (pixels)

- Pixel stability:
  - 1% from ratio plots and dynamic inefficiencies studies
- Dynamic inefficiency:
  - 0.5% from efficiency plots
- Afterglow:
  - 0.5% from analysis of different filling schemes
- Geometrical acceptance:
  - 0.3% from bias study

# Difficulty of p-Pb & Pb-p scans (II)

- The standard out-of-the-box (double) Gaussian fits used to describe the beam overlap shape for pp@8TeV describe the data badly
  - Tried a number of variations of the Gaussian theme, among them second Gaussian can contribute with negative sign which improved things a bit
  - Data appeared to be more “squat” than can be comfortably described by Gaussians
- A clear case for .... Supergaussians
  - Mentioned by W. Kozanecki in an earlier meeting of the LHC Lumi Calibration and Monitoring WG
  - They are used in laser physics to describe higher beam modes which make the beam shape either more rectangular or more peaked (Christmas tree distribution) than a Gaussian
  - Supergaussians were used at SLC, see:  
<http://slac.stanford.edu/cgi-wrap/getdoc/slac-pub-6684.pdf>

# Supergaussians

## One dimension modified Gaussian

- Un-normalised

$$\text{ModGauss}(x) = A \exp\left(-\frac{1}{2} \left(\frac{(x - \mu)^2}{\sigma^2}\right)^{1+\frac{\epsilon}{2}}\right)$$

or equivalently

$$\text{ModGauss}(x) = A \exp\left(-\frac{1}{2} \left(\frac{|x - \mu|}{\sigma}\right)^{2+\epsilon}\right)$$

- To normalise

$$A = \frac{2^{-\frac{3+\epsilon}{2+\epsilon}}}{\sigma \Gamma \left[ 1 + \frac{1}{2+\epsilon} \right]}$$

$\Gamma$  is the gamma function

ModGauss is defined for  $\epsilon > -1$

From Witold's presentation:

<https://indico.cern.ch/materialDisplay.py?contribId=8&materialId=slides&confId=236932>